The Novel Silver-Containing Antimicrobial Potentiates Aminoglycoside Activity Against *Pseudomonas aeruginosa.*

Gracious Yoofi Donkor[a], Greg M. Anderson[a], Michael Stadler[a], Patrick Ofori Tawiah[a], Carl D. Orellano[a], Kevin A. Edwards[b] and Jan-Ulrik Dahl[a#]

[a]School of Biological Sciences, Illinois State University, Microbiology, Normal, IL, USA

[b]School of Biological Sciences, Illinois State University, Cell Biology, Normal, IL, USA

RUNNING TITLE: Reactive oxygen species in antimicrobial therapy

[#]Address correspondence to Jan-Ulrik Dahl, email: jdahl1@ilstu.edu, phone: +1-(309)-438-7694

Word count:

Abstract: 248

Importance: 128

Manuscript:

Abstract

The rapid dissemination of antibiotic resistance combined with the decline in the discovery of novel antibiotics represents a major challenge for infectious disease control that can only be mitigated by investments into novel treatment strategies. Alternative antimicrobials including silver have regained interest due to their diverse mechanisms of inhibiting microbial growth. One such example is AGXX, a broad-spectrum antimicrobial that produces highly cytotoxic reactive oxygen species (ROS) to inflict extensive macromolecular damage. Due to connections identified between ROS production and antibiotic lethality, we hypothesized that AGXX could potentially increase the activity of conventional antibiotics. Using the gram-negative pathogen *Pseudomonas aeruginosa*, we screened possible synergistic effects of AGXX on several antibiotic classes. We found that the combination of AGXX and aminoglycosides tested at sublethal concentrations led to a rapid exponential decrease in bacterial survival and restored sensitivity of a kanamycin-resistant *P. aeruginosa* strain. We deciphered elevated ROS production as a significant contributor to the synergy and demonstrated that the addition of ROS scavengers resulted in reduced endogenous ROS levels and increased bacterial survival, while *P. aeruginosa* strains deficient in ROS detoxifying/repair genes were more susceptible to AGXX/aminoglycoside treatment. We further demonstrate that this synergistic interaction was associated with a significant increase in outer and inner membrane permeability, resulting in increased antibiotic influx. Our study also revealed that AGXX/aminoglycoside-mediated killing requires an active proton motive force across the bacterial membrane. Overall, our findings provide an understanding of cellular targets that could be inhibited to increase the activity of conventional antimicrobials.

IMPORTANCE

The emergence of drug-resistant bacteria coupled with the decline in antibiotic development highlights the need for novel alternatives. Thus, new strategies aimed at repurposing conventional antibiotics have gained significant interest. The necessity of these interventions is evident especially in gram-negative pathogens as they are

particularly difficult to treat due to their outer membrane. This study highlights the effectiveness of the silver containing antimicrobial AGXX in potentiating aminoglycoside activities against *P. aeruginosa*. The combination of AGXX and aminoglycosides not only reduces bacterial survival rapidly but also significantly re-sensitizes aminoglycoside-resistant strains. In combination with gentamicin, AGXX induces increased endogenous oxidative stress, membrane damage and iron sulfur cluster disruption. These findings emphasize AGXX's potential as a route of antibiotic adjuvant development and shed light into potential targets to enhance aminoglycoside activity.

Introduction

The spread of antibiotic resistance has now reached a large number of bacterial pathogens and evolved into a pertinent global health challenge (1). Over the past decade, resistance has been reported against all classical antibiotics, including last resort treatments such as polymyxins (2). The resistance crisis is further exacerbated in gram-negative pathogens due to the impermeability of their outer membrane and the extensive arsenal of drug resistance mechanisms that these critters employ. One example of a difficult to treat gram-negative bacterium is the opportunistic pathogen *P. aeruginosa*, a common cause of acute (e.g., wounds, burns) and chronic infections (e.g., diabetic ulcers, cystic fibrosis) (3). *P. aeruginosa* is characterized by its high intrinsic and acquired resistance mechanisms, allowing the pathogen to thrive in the presence of a large number of antibiotics (4).

In light of these challenges, recent studies have focused on alternative treatment strategies to limit bacterial infection and colonization (5, 6). Transition metals, such as silver and copper, have long been recognized for their antimicrobial activities and were already used by the ancient Greeks for would healing (7). Despite its long-standing history and high efficiency against bacteria, the antimicrobial mode of action of silver is poorly understood. Pleiotropic effects have been described and include changes in DNA condensation, membrane alteration and protein damage (7, 8). Silver ions have a particularly high affinity for cysteine thiols, disrupt exposed iron-sulfur clusters of

82 dehydratase enzymes, and replace metal-containing cofactors, thus affecting a wide
83 range of cytoplasmic and membrane proteins (9, 10). More recently, silver derivates have
84 received increased attention in medical applications, e.g. as antimicrobial surface-
85 coatings on catheters and implants to protect against biofilm-forming bacteria and to
86 reduce the risk of nosocomial infections (5, 11). One such promising silver-based
87 antimicrobial with broad-spectrum activity is AGXX. AGXX consists of micro-galvanic
88 elements of silver (Ag) and ruthenium (Ru), which are surface conditioned with ascorbic
89 acid (12, 13). AGXX has been used in the form of a powder and implemented as an
90 electroporated sheet on a variety of surfaces, including steel meshes, ceramics and water
91 pipes, to limit bacterial colonization. AGXX's antimicrobial activity is not entirely
92 dependent on the release of silver ions, but instead is proposed to occur through the
93 generation of reactive oxygen species (ROS), such as hydroxyl radicals and superoxide
94 (13–15). AGXX-generated ROS is produced through a series of redox reactions where
95 the oxidized Ag component is reduced by organic matter and donates electrons to the
96 valent Ru, which subsequently generates superoxide and other toxic ROS (12, 16).
97 Previous studies revealed that, compared to classical silver and other metals, AGXX was
98 significantly more bactericidal against gram-positive bacteria such as *Staphylococcus*
99 *aureus* and *Enterococcus faecalis*, although no mechanistic details were provided (12,
100 13). Surprisingly, the antimicrobial effects of AGXX on gram-negative pathogens remain
101 largely unexplored.

102 Compounds that generate ROS and/or stimulate endogenous oxidative stress in bacteria
103 have gained interest as potential antibiotic adjuvants (17). Adjuvants increase the efficacy
104 of antibiotics by targeting metabolic processes or cellular networks that ultimately lead to
105 a synergistic increase in antibiotic potency (18). A classic example for the synergy
106 between adjuvants and antibiotic is the combination of amoxicillin, a beta-lactam
107 antibiotic, and clavulanic acid. Due to clavulanic acid's high affinity for beta-lactamase
108 enzymes, its combination with the beta-lactam antibiotics, such as amoxicillin,
109 synergistically potentiate their activity against penicillin-resistant bacteria (19). The
110 hypothesis behind the synergistic effects of ROS-generating or -inducing compounds is
111 based on the multimodal action of these compounds, which could potentially disrupt
112 bacterial targets necessary for the defense of antibiotics (20). Recent studies on the

113 bactericidal mode of action of aminoglycoside, fluoroquinolone and beta-lactam
114 antibiotics have proposed increased endogenous ROS stress as an additional
115 mechanism for bacterial killing (5, 20, 21). Notably, activation of the bacterial envelope
116 stress response, hyperactivation of the electron transport chain, and damage of iron sulfur
117 clusters have been shown to contribute to an increase in endogenous ROS level (5).
118 Although these findings are controversial, extensive evidence has been presented for the
119 integral role of ROS-mediated damage in antibiotic-induced cell death (6). More
120 importantly, recent studies employing ROS-generating compounds have reported
121 promising results on their potential in sensitizing a wide variety of multidrug-resistant
122 bacteria to both bactericidal and bacteriostatic antibiotics (5).

123 Given that AGXX's proposed mode of action is based on ROS production and studies
124 with focus on evaluating potential synergistic effects of AGXX on conventional antibiotics
125 are lacking, we started to investigate possible potentiating effects of AGXX on members
126 of several antibiotic classes, using the *P. aeruginosa* strain PA14 as a model. Exploring
127 potential synergies between AGXX and antibiotics could provide viable answers to the
128 antimicrobial discovery drought, for instance by reducing the minimal inhibitory
129 concentrations of conventional antibiotics required for treatment or possibly overriding
130 and/or delaying antibiotic resistance development (22). By exposing PA14 to sublethal
131 concentrations of AGXX and the antibiotics of interest alone and in combination, we found
132 that bacterial survival was exponentially reduced when the cells were exposed to
133 combinations of AGXX and aminoglycoside antibiotics. Moreover, combined treatment of
134 both compounds re-sensitized a kanamycin resistant PA14 strain to sublethal
135 concentrations of the antibiotic. We further demonstrate that the combined treatment of
136 AGXX and aminoglycosides resulted in increased endogenous oxidative stress and a
137 subsequent disruption of iron homeostasis, potentially providing an explanation for the
138 elevated ROS level. The synergy was associated with a significant increase in outer and
139 inner membrane permeability, which facilitates antibiotic influx. Moreover, our studies
140 revealed that the synergy between AGXX and aminoglycosides relies on an active proton
141 motive force across the bacterial membrane.

142

143 ## Results

144 **AGXX is more efficient in killing *P. aeruginosa* than silverdene and silver nitrate.**
145 Studies with silver ions suggest that gram-negative bacteria are more susceptible than
146 gram-positive bacteria (23). In this study, we investigated the effect of AGXX on *P.*
147 *aeruginosa* using PA14 as model strain. To compare the effective antimicrobial
148 concentrations of different AGXX formulations against PA14, we first performed survival
149 analyses in the presence and absence of AGXX383, AGXX394, AGXX720C, and
150 AGXX823, respectively. While these AGXX formulations all consist of the galvanized
151 silver/ruthenium complex, they differ in various aspects such as silver ratio, particle size,
152 and production procedure, which may affect their antimicrobial activity. Our time killing
153 assays revealed that AGXX383 and AGXX394 have comparable antimicrobial activities
154 against PA14 and are considerably more potent in inhibiting PA14 growth and survival
155 compared to AGXX823 and AGXX720C (**Supplementary FIG S1**). Silver derivates have
156 received increased attention in medical applications, e.g. as antimicrobial surface-
157 coatings on catheters that protect from biofilm-forming bacteria and reduce the risk of
158 nosocomial infections (24). Moreover, silver is used in topicals to prevent and/or treat
159 infections in wounds (25). One such example is silver sulfadiazine (silverdene), the gold
160 standard for treating and preventing *P. aeruginosa* infections in burn wound patients (26).
161 However, silverdene is associated with complications such as allergic reactions to the
162 sulfadiazine moiety emphasizing the need for novel treatment therapies (26). To compare
163 the antimicrobial activities of AGXX394, silver nitrate and silverdene, we conducted
164 survival studies of PA14 in the presence and absence of 25 μg/ml of each compound.
165 Survival of PA14 was highly compromised when cells were exposed to AGXX394 (**Fig.1**).
166 A direct comparison of the killing efficiencies between AGXX394 and silverdene and silver
167 nitrate after 3 hours of treatment revealed a ~1-log and 2-log higher bactericidal activity
168 for AGXX394, respectively, potentially making AGXX an attractive treatment/prevention
169 alternative (**Fig. 1).**

170 ***AGXX exponentially increases the activity of aminoglycosides against P.***
171 ***aeruginosa.*** Our next goal was to determine whether inhibitors of DNA replication
172 (fluoroquinolones), cell wall biosynthesis (β-lactams), folate biosynthesis, membrane

173 integrity (polymyxins), and translation (aminoglycosides) show increased bactericidal
174 activity against *P. aeruginosa* when they were combined with AGXX. To investigate
175 AGXX's potential as a stimulating agent for antibiotic activity, we used AGXX720C, a
176 formulation with lower antimicrobial activity that allowed us to control dosage of AGXX
177 more reliably (**Supplementary FIG S1**). We determined the minimal inhibitory
178 concentrations (MIC) of AGXX720C and ten members of five different antibiotic classes
179 in PA14, which were cultivated under aerobic conditions in Mueller-Hinton broth
180 (**Supplementary Table S1**). Using time killing assays, we exposed PA14 to sublethal
181 concentrations of AGXX720C (75 µg/ml), the indicated antibiotics, and their combinations
182 at the same sublethal concentrations that were used for the individual treatments,
183 respectively. We monitored colony forming units counts every 60 min over a time course
184 of three hours (**Supplementary FIG S2**) and calculated the percent survival for each
185 sample at the 3-hour time point relative to the untreated control (**FIG 2)**. None of the
186 individual treatments with either 75 µg/ml AGXX720C or any of the antibiotics resulted in
187 substantial killing of PA14 (**FIG 2; Supplementary FIG S2**). The combination of 75 µg/ml
188 AGXX720C with 35 ng/ml ciprofloxacin and 100 ng/ml norfloxacin, respectively, resulted
189 in PA14 survival comparable to the individual treatments suggesting that AGXX does not
190 potentiate the bactericidal activities of fluoroquinolones against PA14 (**FIG 2A;**
191 **Supplementary FIG S2A, B**). Likewise, the combined treatments of AGXX720C and 78
192 µg/ml carbenicillin, 0.156 µg/ml imipenem, or 125 µg/ml trimethoprim did not significantly
193 change PA14 survival compared to their individual treatments (**FIG 2B, C;**
194 **Supplementary FIG S2C**). On the other hand, we found that the bactericidal activity of
195 the membrane targeting antibiotic polymyxin B was increased by the presence of
196 AGXX720C as evidenced by a 1-log reduction in PA14 survival as compared to AGXX or
197 polymyxin B alone, which each caused less than 5% killing (**FIG 2D; Supplementary FIG**
198 **S2D**). However, we observed the most drastic decrease in PA14 survival when
199 AGXX720C was combined with a member of aminoglycoside antibiotics, even at
200 concentrations far below the MIC. Co-treatment of AGXX720C with 0.4 µg/ml gentamicin
201 (Gm) (0.2x MIC) reduced PA14 survival by as much as 4 logs after three hours of
202 treatment (**FIG 2E; Supplementary FIG S2E**), while combinations of AGXX720C with 2
203 µg/ml amikacin (0.27x MIC), 1 µg/ml tobramycin (0.4x MIC), or 3 µg/ml streptomycin

204 (0.15x MIC) caused up to 3 log reduction in survival (**FIG 2E, Fig Supplementary S2F-**
205 **H**).

206 **AGXX increases the sensitivity of *P. aeruginosa* strain PA14 to kanamycin.**
207 Considering the significant increase in lethality upon concurrent exposure of PA14 to
208 AGXX720C and aminoglycosides, we sought to determine whether the addition of
209 AGXX720C could reintroduce sensitivity in aminoglycoside-resistant *P. aeruginosa*
210 strains. Like many other *P. aeruginosa* strains, PA14 is intrinsically resistant to many
211 different antibiotics, including the aminoglycoside kanamycin. Under the conditions
212 tested, our PA14 strain showed a MIC of 240 µg/ml for kanamycin. We then exposed
213 PA14 to 75 µg/ml AGXX720C, 50 µg/ml kanamycin, or a combination of 75 µg/ml
214 AGXX720C and 50 µg/ml kanamycin and determined their survival over the time course
215 of 3 hours as described before. As early as 60 minutes post treatment, the combination
216 of AGXX720C and kanamycin reduced colony survival by ~1.5 log, which increased to
217 about 4 log (10,000-fold) difference in survival after 3 hours (**FIG 3**). In summary, we
218 conclude from our data that AGXX potentiates the activity of a wide range of
219 aminoglycoside antibiotics, potentially making aminoglycoside-resistant *P. aeruginosa*
220 strains more sensitive again.

221 ***The combination of sublethal concentrations of AGXX and aminoglycosides***
222 ***increases ROS formation and causes DNA damage and protein aggregation.***
223 AGXX's main antimicrobial mode of action is mediated by the generation of ROS (12, 16)**.**
224 Increased endogenous oxidative stress has also been linked to the lethality of
225 aminoglycosides and other bactericidal antibiotics (27, 28). It may therefore be possible
226 that a disruption in the redox balance during antibiotic exposure increases lethality by
227 amplifying the adventitious generation of ROS by antibiotics. Thus, we quantified
228 intracellular ROS levels using the redox-sensitive molecular probe
229 dichlorodihydrofluorescein diacetate (H_2DCFDA). H_2DCFDA has been extensively
230 demonstrated to detect various ROS, including peroxides as well as peroxyl- and hydroxyl
231 radicals (29). We treated exponentially growing PA14 for 60 min with sublethal
232 concentrations of Gm (0.25 µg/ml), AGXX720C (50 µg/ml), or their combination and
233 compared H2DCFDA fluorescence in each sample to the untreated control. Individual

234 treatments with either Gm or AGXX720C did not result in a significant increase in
235 H_2DCFDA fluorescence, excluding the possibility that substantial amounts of ROS were
236 formed at these sublethal concentrations (**FIG 4A**). However, when applied in
237 combination, we observed an 8-fold increase in H_2DCFDA fluorescence indicative of
238 increased ROS production under these conditions. Pre-treatment of PA14 with the ROS
239 scavenger thiourea (30) or the hydrogen peroxide-detoxifying enzyme catalase resulted
240 in a significant decline in H_2DCFDA fluorescence (**FIG 4A**) as well as restored PA14
241 survival by 2- to 4-log (**FIG 4B; Supplementary FIG S3A**). Thus, our data suggest that
242 the high antimicrobial activity of the combinational treatment can at least in parts be
243 explained by increased ROS formation. However, H_2DCFDA is rather unspecific and
244 detects numerous ROS compounds. We therefore followed up on our observation with
245 the use of additional, more specific ROS-detecting fluorescent dyes. We used the
246 boronate-based peroxy orange 1 (PO1) dye as well as hydroxyphenyl fluorescein (HPF)
247 to examine intracellular concentrations of hydrogen peroxide and hydroxyl radical levels,
248 respectively. After 1 hour of treatment, we detected a significant shift in PO1 and HPF
249 fluorescence, indicating that both hydrogen peroxide and hydroxyl radicals are produced
250 in AGXX720C/Gm-treated PA14 (**FIG 4C, D; Supplementary FIG S3B, C**).

251 Microorganisms have evolved intricate systems to maintain and restore a balanced redox
252 homeostasis and repair ROS-mediated damage [recently reviewed in (5, 31–35)].
253 Proteins and nucleic acids represent two of the most susceptible targets of ROS (36, 37).
254 To test whether the elevated ROS production causes macromolecular damage in PA14
255 cells treated with Gm and AGXX alone and in combination, we analyzed the transcript
256 level of *ipbA* and *sulA,* two genes that have previously been shown to be upregulated in
257 the presence of oxidants such as hypochlorous acid. *ibpA* encodes a molecular
258 chaperone, which plays a significant role in protecting bacteria from proteotoxic stressors
259 (40). *sulA* encodes the cell division inhibitor SulA, which is part of the SOS response and
260 induced when the cell experiences DNA damage (41). We exposed exponentially growing
261 PA14 cells to sublethal concentrations of AGXX720C, Gm, or the combination thereof for
262 60 min and quantified *ibpA/sulA* mRNA level. While individual treatments with sublethal
263 concentrations of AGXX720C or Gm did not cause significant changes in *ibpA/sulA*
264 expression, their transcript levels were approximately 5-fold (*sulA*) and 100-fold (*ibpA*)

265 increased when PA14 was treated with the combination of AGXX720C and gentamicin,
266 indicating significant macromolecule damage **(FIG 4E)**.

267 ***Antioxidant systems provide protection against ROS-mediated damage caused by***
268 ***a combinational treatment of AGXX and aminoglycosides****.* To further investigate the
269 role of ROS for the synergistic activity between aminoglycosides and AGXX, we tested
270 the susceptibility of PA14 strains with transposon insertions in genes that have previously
271 been identified as major oxidative stress response and/or defense systems. We exposed
272 PA14 transposon mutant strains with defects in *oxyR* (encodes ROS-sensing
273 transcriptional regulator OxyR), *katA* (encodes catalase KatA), *katB* (encodes catalase
274 KatB), and *dps* (encodes an iron acquisition protein in response to oxidative stress) to the
275 combination of AGXX720C (25 µg/ml) and tobramycin (0.25 µg/ml) for 3 hours and
276 compared their colony survival to that of the corresponding wildtype strain PA14 (**FIG 5**).
277 We found that strains deficient in functional copies of *katA* and *dps* showed a little over 1
278 log reduced survival compared to wildtype cells, while no difference in survival was
279 observed for cells lacking the hydrogen peroxide global regulator OxyR and catalase
280 KatB, respectively (**FIG 5**). Taken together, our findings point towards a relevant role that
281 ROS generation plays for the synergistic interaction between aminoglycosides and
282 AGXX.

283 ***The synergy between AGXX and aminoglycosides on PA14 killing is in parts***
284 ***mediated by a disruption in iron homeostasis.*** Fe/S cluster are essential cofactors in
285 various metabolic enzymes, including members of the electron transport chain and the
286 TCA cycle (42). Fe/S cluster are particularly vulnerable to ROS, which negatively impacts
287 the activity of metabolic enzymes and ultimately affects cellular metabolism during
288 periods of oxidative stress. Likewise, silver has been found to disrupt Fe/S clusters in
289 proteins (10), resulting in a cellular increase in free iron, which in turn can stimulate
290 hydroxyl radical formation via Fenton reaction and cause extensive macromolecular
291 damage (7). Given the elevated hydroxyl radical level (**FIG 4D; Supplementary FIG S3C**)
292 and increased susceptibility of a *dps*-deficient strain upon PA14 exposure to the
293 AGXX/Gm combination (**FIG 5**), we wondered whether the increased ROS production
294 impairs the activity of Fe/S cluster-containing enzymes. We prepared cell lysates of the

295 four samples that were prepared as described before and measured the activity of
296 aconitase, an Fe/S-containing enzyme of the TCA cycle, whose activity depends on the
297 presence of the Fe/S-cluster. While individual treatments with sublethal AGXX720C or
298 Gm concentrations had no impact on aconitase activity, exposure to a combination of
299 AGXX720C and Gm resulted in ~75% loss in activity (**FIG 6A**). The loss in aconitase
300 activity could be explained by the release of iron atoms, as it occurs during Fe/S cluster
301 oxidation under superoxide and hydrogen peroxide stress (42, 43). To test the role of free
302 iron for the synergistic effect between AGXX720C and aminoglycosides, we treated PA14
303 with the iron chelator 2',2' bipyridyl prior to their exposure to sublethal concentrations of
304 AGXX720C and Gm. Indeed, we found that PA14 survival was less impaired when cells
305 had been treated with 2',2' bipyridyl prior to the presence of the AGXX720C/Gm cocktail
306 **(FIG 6B).** Overall, our data suggest an important role of free iron for the ROS-mediated
307 toxicity of aminoglycoside exposure when in synergy with AGXX.

308 ***Combined AGXX and aminoglycoside treatment induces significant membrane***
309 ***damage.*** Considering the exponential and rapid increase in killing when aminoglycosides
310 were administered in combination with AGXX, we were interested in the underlying
311 reasons for this synergistic relationship. In the initial stages of aminoglycoside uptake, the
312 polycationic aminoglycoside electrostatically interacts with the bacterial outer membrane,
313 displacing membrane divalent cations and inevitably increasing membrane permeability
314 (44). Thus, several compounds with membrane permeabilizing properties have been
315 reported as potent aminoglycoside adjuvants (45, 46). To probe the role of membrane
316 permeability, we evaluated outer membrane disruption using the hydrophobic fluorescent
317 probe N-phenyl-1-napthylamine (NPN), which has diminished fluorescence in the
318 presence of an intact outer membrane. NPN fluorescence significantly increases when
319 the dye is bound to exposed phospholipid groups in a disrupted lipopolysaccharide
320 monolayer (47). We found that in contrast to individual treatments with sublethal
321 AGXX720C and Gm concentrations, a combined treatment significantly increased NPN
322 uptake, resulting in ~7-fold higher NPN fluorescence (**FIG 7A**). Next, we examined the
323 inner membrane permeability of PA14 cells that were subjected to AGXX720C and Gm
324 treatment alone and in combination, using the fluorescent probe propidium iodide (PI).
325 Due to its size and charge, PI can only cross compromised inner membranes where it

326 binds nonspecifically to nucleic acids enhancing its fluorescence exponentially (48).
327 Individual treatments with sublethal AGXX720C and gentamicin concentrations did not
328 result in significantly increased PI fluorescence (**FIG 7B**) suggesting that at these
329 concentrations none of the individual stressors causes significant plasma membrane
330 damage. A combined treatment, however, led to substantially increased PI fluorescence.
331 Our spectrophotometric findings were complemented by fluorescent microscopy analyses
332 of PA14 cells that were treated as described before, washed in PBS, stained with Syto9/PI
333 (live/dead stain), incubated in the dark for 15 minutes at room temperature, mounted onto
334 a glass slide with 1% agarose, and imaged at 60x magnification via inverted confocal
335 microscopy. While the individual treatments with 0.25 µg/ml Gm or 50 µg/ml AGXX720C
336 only caused increased PI fluorescence in very few cells, the number of PI-stained cells
337 was substantially higher in PA14 cells that were treated with a combination of sublethal
338 AGXX720C/Gm concentrations (**FIG 7C**).

339 ***AGXX increases aminoglycoside uptake and lethality through increased activity of***
340 ***the proton motive force (PMF).*** Considering the significance of membrane permeability
341 for aminoglycoside uptake, we reasoned that the increased membrane disruption PA14
342 experiences during a combined treatment of AGXX and aminoglycosides would facilitate
343 intracellular accumulation of aminoglycosides. Using flow cytometry, we evaluated the
344 uptake of Texas-Red-labeled Gentamicin (TR-Gm) in exponentially growing PA14 in the
345 presence or absence of AGXX720C. Treatment of PA14 with a combination of
346 AGXX720C and TR-GM resulted in a significant increase in TR-Gm uptake similar to
347 treatment with the membrane-targeting antibiotic polymyxin B (**FIG 8A, Supplementary**
348 **FIG S4A).** The increased uptake of TR-Gm in the presence of AGXX resulted in a 2.5 log
349 reduction in bacterial survival compared to PA14 that were only exposed to TR-Gm alone
350 **(Supplementary FIG S4B**). Moreover, the secondary and tertiary stage of
351 aminoglycoside import appears to depend on an active membrane potential and occurs
352 therefore only in actively respiring cells (44, 49). As such, increasing cellular respiration
353 or stimulation of membrane potential has been found to increase aminoglycoside lethality.
354 Using the protonophore CCCP, a compound that efficiently inhibits the proton motive
355 force (PMF), we determined whether the synergy between AGXX and aminoglycosides
356 is dependent on the membrane potential. Not surprisingly, PA14 killing by a lethal dose

357 of gentamycin (1 µg/ml) could be reduced by almost 2 logs when the cells were pre-
358 incubated with CCCP (**Supplementary FIG S4C).** Likewise, pretreatment with CCCP
359 restored PA14 survival to a similar degree in the presence of 0.25 µg/ml Gm and 50 µg/ml
360 AGXX720C for three hours **(Fig. 8B).** Surprisingly, combining polymyxin B at 1x MIC and
361 2x MIC with sublethal gentamicin concentrations did not result in increased killing relative
362 to polymyxin B alone **(Fig. S2D)**. Overall, our findings indicate that AGXX's synergistic
363 effect on aminoglycoside lethality does not only involve increased membrane permeability
364 but also requires an active proton motive force across the bacterial membrane.

365

366 ## Discussion

367 In the present study, we provide evidence for a potential suitability of the novel silver
368 containing antimicrobial AGXX as an antibiotic adjuvant with activity on the opportunistic
369 pathogen *P. aeruginosa*. We show that AGXX serves as an efficient tool to potentiate the
370 activity of aminoglycoside antibiotics by reducing bacterial survival up to 50,000-fold.
371 Aside from a 1-log increase in killing found when the ROS-producing Ag/Ru complex was
372 combined with the membrane-targeting antibiotic polymyxin B, AGXX did not influence
373 the activity of antibiotics targeting DNA replication, cell wall synthesis, or folate
374 metabolism **(FIG 2)** raising the possibility that AGXX's potentiating effects could be linked
375 to a malfunction in protein synthesis. AGXX's potentiating effect was not limited to select
376 aminoglycosides but applied to all members tested including gentamicin, streptomycin,
377 amikacin, and tobramycin (**FIG 2**). Additional support for AGXX's stimulating effect on
378 aminoglycoside activity was provided by its ability to re-sensitize a kanamycin resistant
379 *P. aeruginosa* strain (**FIG 3**). Notably, both AGXX and aminoglycoside antibiotics were
380 present at concentrations far below their MICs (0.1-0.3x MIC) indicating that the
381 combination between the compounds was quite powerful with regards to increasing the
382 bactericidal activity of aminoglycosides.

383 Based on our findings, we propose the following model for the synergy between AGXX
384 and aminoglycoside antibiotics (**FIG 9**): The antimicrobial action of AGXX is mediated by
385 superoxide (O_2^-) and hydrogen peroxide (H_2O_2), which are generated in a redox cycle

386 between silver (Ag) and ruthenium (Ru^{x+1}) (15, 16). While the location of AGXX-mediated
387 ROS production was not the focus of his study, we propose that ROS is mainly generated
388 in the extracellular part before the compounds penetrate the cell. This assumption is
389 based on our finding that exogenous addition of catalase was highly effective in reducing
390 ROS level and increasing *P. aeruginosa* survival upon treatment with a combination of
391 AGXX and Gm (**Supplementary FIG S3A**), given that catalase cannot readily cross the
392 bacterial cell envelope. The combination of AGXX and aminoglycosides concertedly
393 increased endogenous ROS levels, including hydrogen peroxide and hydroxyl radicals.
394 Potentially intensified by released silver ions, the increased ROS level may disrupt iron-
395 sulfur clusters in metabolic enzymes such as aconitase, resulting in the release of free
396 iron, which ultimately triggers hydroxyl radical (OH•) formation in a Fenton reaction.
397 Increasing ROS levels can inflict macromolecule damage such as in DNA, proteins, and
398 lipids, as evidenced by *(i)* the increased expression of members of the SOS and heat
399 shock responses, and *(ii)* the possibility that the observed damage on outer and inner
400 membrane is mediated by ROS. In either way, increased ROS production contributes to
401 the enhanced killing of *P. aeruginosa* upon treatment with a combination of AGXX and
402 aminoglycosides. The synergistic effect between AGXX and aminoglycosides is also
403 mediated by an increased uptake and the cellular accumulation of aminoglycosides,
404 which can be attenuated by disrupting the bacterial membrane potential with ionophores
405 such as CCCP.

406 The antimicrobial effects of silver and silver containing agents have been extensively
407 documented (50–52). However, in spite of the increasing use of silver in antimicrobial
408 applications, its mechanism of action remains to be poorly understood (24, 53, 54). Silver
409 along with other ROS inducing agents have been proposed to induce an array of
410 multimodal cytotoxic events, including the mis-metalation of proteins, DNA damage, and
411 imbalanced redox homeostasis, which ultimately disrupt multiple bacterial networks
412 leading to cell death (5, 17, 55). Thus, we investigated whether AGXX, through its
413 multimodal effects as an ROS inducing compound, could increase that activity of
414 conventional antibiotics against *P. aeruginosa*. AGXX itself has been proposed to exert
415 its antimicrobial action through the generation of ROS rather than the release of silver
416 ions. AGXX-mediated ROS production likely starts with the generation of superoxide,

417 which subsequently can be dismutated by cellular superoxide dismutases into hydrogen
418 peroxide (15, 56). Likewise, aminoglycosides have also been posited to induce metabolic
419 alterations that induce endogenous ROS level (57). We found a significant increase in
420 hydrogen peroxide and hydroxyl radical signals upon exposure of PA14 to a combination
421 of AGXX and aminoglycoside as evidenced by increased PO1 and HPF fluorescence
422 **(FIG 4)** and decreased survival of transposon insertion strains defective in KatA and Dps
423 **(FIG 5)**. Surprisingly, a transposon insertion into the *oxyR* gene, encoding the major
424 hydrogen response regulator OxyR, did not show a significant difference in survival
425 relative to the wildtype under combined AGXX/aminoglycoside exposure **(FIG 5)**.
426 However, this is consistent with a previous study on the aminoglycoside potentiating
427 effects of silver nitrate, in which neither *oxyR*-deficient strains nor strains that
428 constitutively express OxyR had significant effects on bacterial survival (58). On the other
429 hand, the overexpression of the H_2O_2 detoxifying gene *ahpF* attenuated the lethality and
430 proteotoxic effects of aminoglycosides, providing evidence for the relevance of hydrogen
431 peroxide in aminoglycoside toxicity (59). Previous studies have demonstrated that
432 pretreatment with antioxidant molecules such as thiourea reduced intracellular hydroxyl
433 radical levels and increased bacterial survival during aminoglycoside and silver stress
434 (17, 28, 60, 61). Consistent with these findings, we made similar observations as the
435 addition of either catalase or thiourea to AGXX-aminoglycoside-treated PA14 resulted in
436 a significant reduction in endogenous ROS level as well as bacterial killing relative to the
437 combined treatment alone **(FIG 4A, B; Supplementary FIG S3A)**. Given that individual
438 AGXX or gentamicin treatments did not result in a significant increase in ROS signals, it
439 is plausible that applying these antimicrobials at concentrations far below the MIC would
440 not induce the physiological/metabolic alterations necessary for aggravating endogenous
441 ROS levels.

442 Considering that both superoxide and silver ions have been reported to destabilize Fe/S
443 cluster proteins resulting in the release of solvent-exposed iron (10, 62), we investigated
444 the effects of individual and combinational treatments with AGXX and/or aminoglycoside
445 antibiotics on the activity of aconitase, an Fe-S cluster containing enzyme. We found
446 aconitase to be extremely sensitive towards exposure to both antimicrobials when
447 administered in combination (**FIG 6A**). Disrupted Fe-S clusters could potentially lead to

448 an increase in intracellular iron levels and subsequent OH• generation through Fenton
449 reaction as it has been demonstrated under hydrogen peroxide stress in ROS-sensitive
450 *E. coli* strains (63). This would explain the significantly higher OH• levels detected in PA14
451 cells that were exposed to a combined AGXX and gentamicin mixture **(FIG 4)**, which could
452 cause significant DNA damage and induce the SOS response. In fact, we found that the
453 combination of sublethal AGXX and gentamicin significantly induced the expression of
454 *sulA,* an SOS response marker of DNA damage **(FIG 4E)**. Likewise, addition of 2',2'
455 bipyridyl resulted in a 1-log increase in bacterial survival when cells were exposed to the
456 toxic cocktail of gentamycin and AAGXX suggesting that free iron contributes to the
457 bactericidal effects **(FIG 6B)**. All in all, our findings highlight the relevance of oxidative
458 stress in the enhancement of antibiotic lethality in *P. aeruginosa* exposed to sub-inhibitory
459 concentrations of AGXX and aminoglycosides.

460 Compared to other gram-negative pathogens, *P. aeruginosa* possesses high intrinsic
461 resistance mechanisms towards a variety of antibiotics (64). This resistance is mediated
462 in part by its extensive arsenal of efflux pumps and significantly lower outer membrane
463 permeability (64). We found that combining AGXX and gentamicin increased both inner
464 and outer membrane permeability in *P. aeruginosa* leading to a subsequent increase in
465 aminoglycoside uptake **(FIG 7, FIG 8)**. Aminoglycosides are polycationic in nature and
466 known to displace divalent cations that cross-bridge lipopolysaccharides, which makes
467 the outer membrane substantially more permeable (65, 66). It is therefore possible that
468 AGXX, much like aminoglycosides, disrupts the outer leaflet of the outer membrane, with
469 the result that lower amounts of aminoglycosides are required to permeabilize *P.*
470 *aeruginosa*. If this was true, we would suspect that the initial stages of aminoglycoside
471 uptake could likely be accelerated causing a more rapid antibiotic influx. Surprisingly, we
472 found that the addition of sublethal polymyxin B concentrations did not affect gentamicin
473 lethality indicating that the mechanism behind the potentiating effects of AGXX extends
474 beyond increased membrane permeability **(FIG S4D)**. We further found that disrupting
475 membrane potential using an ionophore increased bacterial survival under combined
476 AGXX and gentamicin stress **(FIG 8)**, suggesting an important role for the energy
477 dependent phase of aminoglycoside uptake AGXX's potentiating effect. By definition,
478 antibiotic adjuvants do not possess inherent antimicrobial activity (67). Even though

479 AGXX can technically not be defined as an antibiotic adjuvant given its own antimicrobial
480 activity (16), our use of sublethal AGXX concentrations to screen for potentiating effects
481 satisfied this definition. Notably, the antimicrobial properties of silver have been accepted
482 for a long time and taken advantage of in topical ointments such as silverdene cremes to
483 prevent and treat *P. aeruginosa* infections in burn wound patients (26). A comparison to
484 silver nitrate and silver sulfadiazine (silverdene) revealed an increased potency of some
485 of the AGXX formulations resulting in a lower survival rate of PA14 **(FIG 1)**. Moreover,
486 given that antibacterial combination therapies typically involve significantly lower
487 concentrations of the antimicrobials compared to what is needed for individual treatments,
488 such approaches would potentially delay resistance development.

489

490 Materials and Methods

491 **Bacterial strains and growth conditions.** Unless stated otherwise, overnight *P.*
492 *aeruginosa* PA14 strains **(Supplementary Table 2)** were grown under aerobic conditions
493 in Luria-Bertani broth (LB, Millipore Sigma) at 37°C for 16-20 hours at 300 rpm. For
494 subsequent assays, overnight cultures were diluted into Mueller-Hinton broth or 3-(N-
495 morpholino) propanesulfonic acid minimal media containing 0.2% glucose, 1.32 mM
496 K_2HPO_4 and 10 μM thiamine (MOPSg) and incubated at 37 °C at 300 rpm.

497 **Minimum Inhibitory Concentration (MIC).** MIC assays were performed in 96-well plates
498 in a total volume of 200 μl per well. Overnight PA14 cultures were diluted into Mueller-
499 Hinton broth to an OD_{600} of 0.002 and distributed into 96 well plates that contained
500 increasing concentrations of ciprofloxacin, nalidixic acid, carbenicillin, imipenem,
501 trimethoprim, polymyxin B, gentamicin, amikacin, tobramycin, streptomycin, and
502 kanamycin, respectively. Plates were subsequently incubated at 37 °C for 16 hours at
503 300 rpm. MIC assays were performed in duplicates. The MIC is defined as the lowest
504 antibiotic concentration that inhibited growth.

505 **Time Killing Assays.** Overnight PA14 cultures were diluted ~25-fold into Mueller-Hinton
506 broth by normalizing cultures to an OD_{600} = 0.1 in a 6-well sterile cell culture plate.
507 Sublethal concentrations of AGXX720C and antibiotics of interest were added individually

508 and in combination as indicated and plates incubated at 37°C for 3 hours at 150 rpm
509 under aerobic conditions. CCCP and BIP were added 60 minutes prior to
510 AGXX/aminoglycoside treatments whenever indicated. At 1-hour intervals, OD_{600} of
511 cultures were recorded, sample volumes were normalized to the lowest optical density
512 measured, serially diluted in PBS (pH = 7.4) and plated on LB agar to quantify colony
513 forming units (CFU) after 16 hours. Percent survival was calculated as the ratio of
514 surviving colonies from treated to untreated samples.

515 **Intracellular ROS level.** Intracellular ROS levels were quantified using the redox-
516 sensitive dye 2',7'-dichlorodihydrofluorescein diacetate (H_2DCFDA) (Thermofisher
517 Scientific). Exponentially growing PA14 cultures were left untreated or treated with 0.25
518 µg/ml Gm, 50 µg/ml AGXX720C or a combination of both for 1 hour. Samples were
519 collected and normalized to an OD_{600}=1.0. Cells were washed twice, resuspended in
520 prewarmed PBS containing 10 µM H_2DCFDA, and incubated in the dark at 37 °C for 30
521 min before samples were washed twice again in PBS and DCF fluorescence measured
522 at excitation/emission wavelengths of 485/535 nm (Tecan 200 plate reader). To quench
523 cellular ROS, cells were pretreated with 50 mM thiourea prior to the stress treatments.

524 **Quantification of hydrogen peroxide level.** The monoborate fluorescent probe peroxy
525 orange 1 (PO1) was used to measure hydrogen peroxide level. Exponentially growing
526 PA14 cultures were treated with 10 µM PO1 prior to their exposure to 0.25 µg/ml Gm, 50
527 µg/ml AGXX720C, or a combination of both for 1 hour. Cells were washed twice and
528 resuspended in prewarmed PBS. Samples were analyzed using the flow cytometer (BD
529 FACS melody) in the FITC channel (613/18 filter). At least 10,000 events were recorded,
530 and figures generated using FCSlayzer.

531 **Quantification of Hydroxyl radical level.** The fluorescent probe hydroxyphenyl
532 fluorescein (HPF; Invitrogen) was used to determine the amount of cellular hydroxyl
533 radicals produced (68). Exponentially growing PA14 cultures were either left untreated or
534 treated for 1 hour with 0.25 µg/ml Gm, 50 µg/ml AGXX720C, or the combination thereof.
535 Samples were collected and normalized to an OD_{600nm} of 1.0 after washing twice with
536 PBS (pH 7.4). Cells were then stained with 10 µM HPF and incubated in the dark for 30
537 minutes at 37 °C. Cells were washed twice and resuspended in prewarmed PBS.

538 Samples were analyzed using the flow cytometer (BD FACS melody) in the FITC channel
539 (527/32 filter). At least 10,000 events were recorded, and figures generated using
540 FCSlayzer.

541 **Gene expression analyses by qRT-PCR.** Overnight PA14 cultures were diluted into
542 MOPSg media to an OD_{600}=0.1 and grown to mid-log phase (OD_{600nm}=0.3). Cultures were
543 left untreated or treated with 0.25 µg/ml Gm, 50 µg/ml AGXX720C, or the combination
544 thereof for 60 minutes. Transcription was stopped by the addition of an equal volume of
545 ice-cold methanol. Total RNA was extracted from three biological replicates using a
546 commercially available RNA extraction kit (Macherey & Nagel). Remaining DNA was
547 removed using the TURBO DNA-free kit (Thermo Scientific). mRNA was reverse
548 transcribed into cDNA using the PrimeScript cDNA synthesis kit (TaKaRa). qRT-PCRs
549 were set up according to the manufacturer's instructions (Alkali Scientific). Transcript
550 levels of the indicated genes were normalized against transcript levels of the 16S rRNA-
551 encoding *rrsD* gene and relative fold changes in gene expression were calculated using
552 the $2^{-\Delta\Delta CT}$ method (69). The following primer pairs were used for gene amplification: *ipbA*,
553 TTCCGTCATTCCGTAGG & AGGTCTTCTTCCTGG; *sulA,*
554 ACTGTTCCAGGAAGCGTTCT & AGCGAAAGTTCGCTAAAGGC; *rrsD,*
555 TATCAGATGAGCCTAGGTCGGATTA & TTTACAATCCGAAGACCTTCTTCAC.
556

557 **Aconitase Assay.** Exponentially growing PA14 were treated with sublethal
558 concentrations of AGXX720C (100 µg/ml), Gm (0.6 µg/ml) or the combination thereof.
559 Aconitase activity was measured from cell lysates using the Aconitase Assay Kit (Abcam)
560 according to manufacturer's instructions. One unit of aconitase is defined as the amount
561 of enzyme that isomerizes 1 µmol of citrate to isocitrate per min at pH 7.4 and 25 °C.

562 **Outer membrane permeability assay.** The N-phenyl-1-naphthylamine (NPN) uptake
563 assay was used to detect outer membrane damage as described in (70). Exponential
564 phase PA14 were treated with 0.25 µg/ml Gm, 50 µg/ml AGXX720C, a combination
565 thereof. Addition of 2 µg/ml polymyxin B was used as a positive control. Cells were
566 collected after 60 min of treatment, washed, and resuspended to an OD_{600}=0.5 in HEPES-
567 sodium buffer (pH 7.2). 10 µM NPN was added, and samples incubated in the dark for 15

568 min. NPN fluorescence was measured at excitation/emission wavelengths of 350/420 nm.
569 Increased NPN uptake (indicating outer membrane damage) was calculated using the
570 following equation (71):

571 $$NPN\ uptake = \frac{Sample_{+NPN} - Sample_{-NPN}}{Hepes\ Buffer_{+NPN} - Hepes\ Buffer_{-NPN}}$$

572 **Inner membrane disruption assay.** Inner membrane integrity was determined by the
573 cellular uptake of propidium iodide following antimicrobial treatments. Exponentially
574 growing PA14 cells were either left untreated or treated with 0.25 µg/ml Gm, 50 µg/ml
575 AGXX720C, or a combination thereof. Cells were harvested after 1 hour, washed twice,
576 and resuspended in PBS (pH 7.4) at an OD_{600}=0.5. Propidium iodide (Thermo Fisher
577 Scientific) was added to a final concentration of 500 nM and samples incubated in the
578 dark for 30 min. Fluorescence intensities were measured at excitation/emission
579 wavelengths of 535/617 nm. Samples treated with polymyxin B at a sublethal
580 concentration (2 µg/ml) were included as a positive control.

581 **LIVE/DEAD staining.** Exponentially growing PA14 cells were either left untreated or
582 treated with 0.25 µg/ml Gm, 50 µg/ml AGXX720C, or a combination thereof. Cells were
583 harvested after 1 hour, washed twice, and resuspended in PBS (pH 7.4) at an OD_{600}=0.2.
584 Samples were stained with SYTO9 (6µM) and PI (30 µM) and incubated in the dark for
585 15 min at room temperature**.** Cells were then transferred onto a glass slide and covered
586 with 1% agarose prior to visualization using a Leica SP2 confocal microscope. Samples
587 treated with polymyxin B at a sublethal concentration (2 µg/ml) were included as a positive
588 control.

589 **Texas Red-Gentamicin Uptake Assay**. Texas Red-succinimidyl ester (Invitrogen) was
590 dissolved to a final concentration of 20 mg/ml in high quality anhydrous N,N-
591 dimethylformamide at 4 °C (72). Gm was dissolved in 100 mM K_2CO_3 (pH 8.5) to a final
592 concentration of 10 mg/ml at 4 °C. 20 ul Texas Red was slowly added dropwise to 700 ul
593 Gm to allow for the conjugation reaction to obtain the Texas-Red labeled gentamicin (TR-
594 Gm) (72). The TR-Gm conjugate was diluted in water and stored at -20 °C protected from
595 light. Exponentially growing PA14 cells were first treated with 1 µg/ml TR-Gm followed by
596 exposure to either 50 µg/ml AGXX720C or 2 µg/ml polymyxin B (positive control). After 1

597 hour incubation in the dark at 37 °C, cells were collected and analyzed in the flow
598 cytometer (BD FACS melody) using the 697/58 filter. At least 10,000 events were
599 recorded, and figures generated using FCSlayzer.

600 **Statistical analyses:** All statistical analyses were performed in GraphPad prism version
601 8.0.

602

603 ## ACKNOWLEDGEMENTS

604 This work was supported by the NIAID grant R15AI164585 and the Illinois State
605 University Pre-Tenure Faculty Initiative Grant (to J.-U. D.). G.Y.D. was supported by
606 Weigel and Mockford-Thompson grants by the Phi-Sigma Biological Sciences Honors
607 Society. G.M.A. and C.D.O. were supported by the Illinois State University Undergraduate
608 Research Support Program. Dr. Uwe Landau and his team from Largentec GmbH are
609 acknowledged for scientific discussion and providing the AGXX formulations. We also
610 thank Sadia Sultana for critically proof-reading the manuscript and providing invaluable
611 feedback. Figure 9 was generated with Adobe Illustrator.

612

613 ## FIGURE LEGENDS

614 **FIG 1 AGXX394 is more efficient in killing *P. aeruginosa* than silverdene and silver**
615 **nitrate.** Overnight PA14 cultures were diluted ~25-fold into MOPSg media (OD_{600}=0.1)
616 and treated for three hours with 25 µg/ml $AgNO_3$ (black symbol), silverdene (grey symbol),
617 and AGXX394 (red symbol), respectively. Colony survival was evaluated every hour by
618 serially diluting samples and plating them onto LB agar. Percent survival was calculated
619 relative to the untreated control (*n=4, ± S.D).*

620 **FIG 2 AGXX exponentially increases the activity of aminoglycosides against *P.***
621 ***aeruginosa*.** Overnight PA14 cultures were diluted ~25-fold (OD_{600}=0.1) into Mueller-
622 Hinton media and exposed to 75 µg/ml AGXX720 (black bars), a sublethal concentration
623 of the indicated antibiotic (grey bar), or the combined treatment of both (red bars) for 3
624 hours. Samples were taking every 60 min, serial diluted, plated on LB agar, and incubated

625 for 20 hours for CFU counts. Percent survival was calculated relative to the untreated
626 control for: **(A)** 35 ng/ml ciprofloxacin and 100 ng/ml nalidixic acid, respectively; **(B)** 78
627 µg/ml carbenicillin and 0.156 µg/ml imipenem, respectively; **(C)** 125 µg/ml trimethoprim;
628 **(D)** 1.5 µg/ml polymyxin B; and **(E)** 0.4 µg/ml gentamicin, 2.0 µg/ml amikacin, 1.0 µg/ml
629 tobramycin, and 3 µg/ml streptomycin, respectively. All experiments were performed in at
630 least three biological replicates and error bars represent mean ± SD. * $p < 0.05$, ** $p <$
631 0.01, *** $p < 0.001$ (Student's t test, calculated relative to cultures treated with antibiotics
632 alone).

633 **FIG 3 AGXX increases the sensitivity of *P. aeruginosa* strain PA14 to kanamycin.**
634 Overnight PA14 cultures were diluted ~25-fold into Mueller-Hinton media (OD_{600}=0.1) and
635 either left untreated or exposed to 75 µg/ml AGXX720C, 50 µg/ml kanamycin, or the
636 combination thereof for 3 hours. Samples were taken every 30 minutes, serial diluted and
637 plated on LB agar for CFU counts, (*n=4, ± S.D)*.

638 **FIG 4 The combination of sublethal concentrations of AGXX and aminoglycosides**
639 **increases ROS formation and causes DNA damage and protein aggregation.** Mid-
640 log PA14 cells were treated with sublethal concentrations of Gm (0.25 µg/ml), AGXX720C
641 (50 µg/ml), the combination thereof, or left untreated. **(A)** Intracellular ROS levels were
642 quantified by H_2DCFDA fluorescence. 50mM thiourea was used as a ROS quencher (*n=3,*
643 *± S.D)*. **(B)** Samples were serially diluted in PBS after 60 min of incubation, spot-titered
644 onto LB agar and incubated for 20 hours. One representative of three independent
645 experiments with similar outcomes. **(C, D)** Cells were strained with **(C)** 10 µM peroxy-
646 orange 1 (PO1) and **(D)** 10µM hydroxyphenyl fluorescein (HPF) for 60 min and
647 fluorescence was measured via flow cytometry (*n=3, ± S.D)*. **(E)** The induction of *sulA*
648 (white bar) and *ibpA* (black bar) transcript levels was determined by qRT-PCR. Gene
649 expression was normalized to the housekeeping gene *rrsD* and calculated as fold
650 changes based on expression levels in the untreated control (*n=3, ± S.D.*). One-way
651 ANOVA, Dunnett's posttest; *ns=p>0.05,* * $p < 0.05$, ** $p < 0.01$, *** $p < 0.001$, **** $p <$
652 0.0001.

653 **FIG 5 Antioxidant systems provide protection against ROS-mediated damage**
654 **caused by a combinational treatment of AGXX and aminoglycosides.** Overnight

655 cultures of PA14 wildtype, Δ*oxyR,* Δ*katA,* Δ*katB* and Δ*dps* were diluted into MOPSg to an
656 OD_{600}=0.01 and grown under aerobic conditions until OD_{600}=0.1. Cultures were either left
657 untreated (grey bars) or treated with a combination of 0.25 µg/ml tobramycin and 25 µg/ml
658 AGXX720C (white bars). Bacterial survival was quantified after two hours by serially
659 diluting cells in PBS and plating on LB agar for 20 hours at 37°C (*n=3,* ± *S.D*). Student t-
660 test, * $p < 0.05$).

661 **FIG 6 The synergy between AGXX and aminoglycosides on PA14 killing is in parts**
662 **mediated by a disruption in iron homeostasis.** Overnight PA14 cultures were diluted
663 into MOPSg and incubated under aerobic conditions until exponential phase was
664 reached. **(A)** Cells were left untreated or treated with 100 µg/ml AGXX720C, 0.6 µg/ml
665 Gm, or the combination thereof for 1 hour. Aconitase activities were determined in crude
666 extracts (*n=4,* ± *S.D*). One-way ANOVA, Dunnett's posttest; *ns=p>0.05,* ** $p < 0.01$. **(B)**
667 Cultures were either left untreated (white square) or treated with 0.25 µg/ml Gm (white
668 diamond), 50µg/ml AGXX720C (white circle), or the combination thereof (white triangle)
669 for three hours. Survival was determined each hour by serially diluting samples in PBS
670 and plating onto LB agar for overnight growth. The impact of free iron on the increased
671 killing by AGXX/Gm cotreatments was tested by the absence (white triangle) and
672 presence (black diamonds) of 125 µM 2',2' bipyridyl (*n=3,* ± *S.D.*). Student's t test,
673 *=p<0.05).

674 **FIG 7 Combined AGXX and aminoglycoside treatment induces significant**
675 **membrane damage.** PA14 cells grown to mid-log phase in MOPSg media were left
676 untreated or treated with sublethal concentrations of Gm (0.25 µg/ml), AGXX720C
677 (50µg/ml), and the combination thereof. Cells were harvested after 1 hour of treatment,
678 washed in PBS, and stained with **(A)** 10 µM N-phenyl-1-naphthylamine (NPN) dye, and
679 **(B)** 0.5 µM propidium iodide (PI). Fluorescence intensities were determined at
680 excitation/emission wavelengths of **(A)** 350/420 nm and **(B)** 535/617 nm, respectively,
681 (*n=4,* ± *S.D.*). One-way ANOVA, Dunnett's posttest; *ns=p>0.05,* * $p < 0.05$, **** $p <$
682 0.0001. **(C)** Samples were washed in PBS, stained with PI/Syto9, incubated in the dark
683 for 15 minutes at room temperature, mounted onto a glass slide with 1% agarose, and

684 imaged at 60x magnification via inverted confocal microscopy. One representative of
685 three independent experiments with similar outcomes.

686 **FIG 8 AGXX increases aminoglycoside uptake and lethality through increased**
687 **activity of the proton motive force (PMF). (A)** Mid-log PA14 cells were treated with 1.0
688 µg/ml TR-Gm, 1.0 µg/ml TR-Gm + 50 µg/ml AGXX720C, and 1.0 µg/ml TR-Gm + 2.0
689 µg/ml polymyxin B (PMB) for 1 hour, respectively. TR-Gm uptake was measured via flow
690 cytometry. **(B)** Mid-log phase PA14 were left untreated (control) or exposed to 0.25 µg/ml
691 Gm, 50 µg/ml AGXX720C or 0.25 µg/ml Gm + 50 µg/ml AGXX720C for 3 hours. Samples
692 were serial diluted, plated on LB agar, and incubated for 20 hours for CFU counts. To test
693 the impact of the PMF on the killing of a combination of AGXX and aminoglycosides,
694 PA14 were pretreated with or without 50 µM carbonyl cyanide *m*-chlorophenyl hydrazone
695 (CCCP) prior to AGXX/Gm exposure *(n=3, ± S.D.)*. Student's t test, ** $p<0.01$.

696 **FIG 9 Proposed model for the synergy between AGXX and aminoglycoside**
697 **antibiotics.** The antimicrobial action of AGXX is mediated by superoxide (O_2^-) and
698 hydrogen peroxide (H_2O_2), which are generated in a redox cycle between silver (Ag) and
699 ruthenium (Ru^{x+1}). The combination of AGXX and aminoglycosides concertedly increases
700 endogenous ROS levels. Potentially facilitated by a release of silver ions, the increased
701 ROS level may disrupt iron-sulfur clusters in metabolic enzymes such as aconitase,
702 resulting in the release of free iron, which ultimately triggers hydroxyl radical (OH•)
703 formation in a Fenton reaction. Increasing ROS levels can inflict macromolecule damage
704 such as DNA damage and protein aggregation, contributing to increased killing as
705 observed for *P. aeruginosa* that were treated with a combination of AGXX and
706 aminoglycosides. The synergistic effect between AGXX and aminoglycosides is also
707 mediated by an increased uptake and the cellular accumulation of aminoglycosides,
708 which can be attenuated by disrupting the bacterial membrane potential with ionophores
709 such as CCCP.

710

711 ## References

712 1. Llor C, Bjerrum L. 2014. Antimicrobial resistance: risk associated with antibiotic
713 overuse and initiatives to reduce the problem. Therapeutic advances in drug safety
714 5:229–41.
715 2. Spellberg B. 2014. The future of antibiotics. Critical Care 18:228.
716 3. Turner KH, Everett J, Trivedi U, Rumbaugh KP, Whiteley M. 2014. Requirements for
717 Pseudomonas aeruginosa Acute Burn and Chronic Surgical Wound Infection. PLOS
718 Genetics 10:e1004518.
719 4. Pang Z, Raudonis R, Glick BR, Lin TJ, Cheng Z. 2019. Antibiotic resistance in
720 Pseudomonas aeruginosa: mechanisms and alternative therapeutic strategies.
721 Biotechnology Advances 37:177–192.
722 5. Chopra I, Hesse L, O'Neill AJ. 2002. Exploiting current understanding of antibiotic
723 action for discovery of new drugs. Symposium series (Society for Applied
724 Microbiology) 31:4S-15S.
725 6. Shang D, Liu Y, Jiang F, Ji F, Wang H, Han X. 2019. Synergistic Antibacterial Activity
726 of Designed Trp-Containing Antibacterial Peptides in Combination With Antibiotics
727 Against Multidrug-Resistant Staphylococcus epidermidis. Frontiers in Microbiology
728 0:2719.
729 7. Barras F, Aussel L, Ezraty B. 2018. Silver and antibiotic, new facts to an old story.
730 Antibiotics 7:1–10.
731 8. GA S, SE P. 2010. Antibacterial activity of nanosilver ions and particles.
732 Environmental science & technology 44:5649–5654.

733 9. Liau SY, Read DC, Pugh WJ, Furr JR, Russell AD. 1997. Interaction of silver nitrate
734 with readily identifiable groups: Relationship to the antibacterial action of silver ions.
735 Letters in Applied Microbiology 25:279–283.
736 10. Xu FF, Imlay JA. 2012. Silver(I), Mercury(II), Cadmium(II), and Zinc(II) Target
737 Exposed Enzymic Iron-Sulfur Clusters when They Toxify Escherichia coli. Applied
738 and Environmental Microbiology 78:3614.
739 11. Church D, Elsayed S, Reid O, Winston B, Lindsay R. 2006. Burn wound infections.
740 Clinical Microbiology Reviews 19:403–434.
741 12. Clauss-Lendzian E, Vaishampayan A, de Jong A, Landau U, Meyer C, Kok J,
742 Grohmann E. 2018. Stress response of a clinical Enterococcus faecalis isolate
743 subjected to a novel antimicrobial surface coating. Microbiological Research 207:53–
744 64.
745 13. Van Loi V, Busche T, Preuß T, Kalinowski J, Bernhardt J, Antelmann H. 2018. The
746 AGXX® antimicrobial coating causes a thiol-specific oxidative stress response and
747 protein s-bacillithiolation in staphylococcus aureus. Frontiers in Microbiology 9:1–15.
748 14. Sobisch LY, Rogowski KM, Fuchs J, Schmieder W, Vaishampayan A, Oles P,
749 Novikova N, Grohmann E. 2019. Biofilm forming antibiotic resistant gram-positive
750 pathogens isolated from surfaces on the international space station. Frontiers in
751 Microbiology 10:1–16.
752 15. Linzner N, Antelmann H. 2021. The Antimicrobial Activity of the AGXX® Surface
753 Coating Requires a Small Particle Size to Efficiently Kill Staphylococcus aureus.
754 Frontiers in Microbiology 12.

755 16. Guridi A, Diederich AK, Aguila-Arcos S, Garcia-Moreno M, Blasi R, Broszat M,
756 Schmieder W, Clauss-Lendzian E, Sakinc-Gueler T, Andrade R, Alkorta I, Meyer C,
757 Landau U, Grohmann E. 2015. New antimicrobial contact catalyst killing antibiotic
758 resistant clinical and waterborne pathogens. Materials Science and Engineering C
759 50:1–11.
760 17. Morones-Ramirez J, Winkler JA, Spina CS, Collins JJ. 2013. Silver enhances
761 antibiotic activity against gram-negative bacteria. Science Translational Medicine 5.
762 18. Kalan L, Wright GD. 2011. Antibiotic adjuvants: multicomponent anti-infective
763 strategies. Expert Reviews in Molecular Medicine 13.
764 19. Huttner A, Bielicki J, Clements MN, Frimodt-Møller N, Muller AE, Paccaud J-P,
765 Mouton JW. 2020. Oral amoxicillin and amoxicillin–clavulanic acid: properties,
766 indications and usage. Clinical Microbiology and Infection 26:871–879.
767 20. Brynildsen MP, Winkler JA, Spina CS, MacDonald IC, Collins JJ. 2013. Potentiating
768 antibacterial activity by predictably enhancing endogenous microbial ROS
769 production. Nature biotechnology 31:160.
770 21. Foti JJ, Devadoss B, Winkler JA, Collins JJ, Walker GC. 2012. Oxidation of the
771 guanine nucleotide pool underlies cell death by bactericidal antibiotics. Science
772 336:315–319.
773 22. Soothill G, Hu Y, Coates A. 2013. Can We Prevent Antimicrobial Resistance by
774 Using Antimicrobials Better? Pathogens 2013, Vol 2, Pages 422-435 2:422–435.
775 23. Feng QL, Wu J, Chen GQ, Cui FZ, Kim TN, Kim JO. 2000. A mechanistic study of
776 the antibacterial effect of silver ions on Escherichia coli and Staphylococcus aureus.
777 Journal of Biomedical Materials Research 52:662–668.

24. Silver S, Phung LT, Silver G. 2006. Silver as biocides in burn and wound dressings and bacterial resistance to silver compounds. Journal of Industrial Microbiology and Biotechnology 33:627–634.
25. Egger S, Lehmann RP, Height MJ, Loessner MJ, Schuppler M. 2009. Antimicrobial Properties of a Novel Silver-Silica Nanocomposite Material. Applied and Environmental Microbiology 75:2973–2976.
26. Fuller FW. 2009. The side effects of silver sulfadiazine. J Burn Care Res 30:464–470.
27. Kohanski MA, Tharakan A, Lane AP, Ramanathan M. 2016. Bactericidal Antibiotics Promote Reactive Oxygen Species Formation and Inflammation in Human Sinonasal Epithelial Cells. International forum of allergy & rhinology 6:191.
28. Kohanski MA, Dwyer DJ, Hayete B, Lawrence CA, Collins JJ. 2007. A Common Mechanism of Cellular Death Induced by Bactericidal Antibiotics. Cell 130:797–810.
29. Kim H, Xue X. 2020. Detection of Total Reactive Oxygen Species in Adherent Cells by 2',7'-Dichlorodihydrofluorescein Diacetate Staining. Journal of visualized experiments : JoVE 2020:1–5.
30. Kelner MJ, Bagnell R, Welch KJ. 1990. Thioureas react with superoxide radicals to yield a sulfhydryl compound. Explanation for protective effect against paraquat. Journal of Biological Chemistry 265:1306–1311.
31. Imlay JA. 2008. Cellular defenses against superoxide and hydrogen peroxide. Annu Rev Biochem 77:755–776.
32. Gray MJ, Wholey W-Y, Jakob U. 2013. Bacterial Responses to Reactive Chlorine Species. Annual Review of Microbiology 67:141–160.

801 33. Varatnitskaya M, Degrossoli A, Leichert LI. 2021. Redox regulation in host-pathogen
802 interactions: thiol switches and beyond. Biological Chemistry 402:299–316.
803 34. Sultana S, Foti A, Dahl J-U. 2020. Bacterial Defense Systems against the
804 Neutrophilic Oxidant Hypochlorous Acid. Infection and Immunity 88:e00964-19.
805 35. Dahl J-U, Gray MJ, Jakob U. 2015. Protein Quality Control Under Oxidative Stress
806 Conditions. J Mol Biol 427:1549–1563.
807 36. Ezraty B, Gennaris A, Barras F, Collet JF. 2017. Oxidative stress, protein damage
808 and repair in bacteria. Nature Reviews Microbiology 2017 15:7 15:385–396.
809 37. Cooke MS, Evans MD, Dizdaroglu M, Lunec J. 2003. Oxidative DNA damage:
810 mechanisms, mutation, and disease. The FASEB Journal 17:1195–1214.
811 38. Groitl B, Dahl J-U, Schroeder JW, Jakob U. 2017. Pseudomonas aeruginosa
812 defense systems against microbicidal oxidants. Molecular Microbiology 106:335–
813 350.
814 39. Sultana S, Crompton ME, Meurer K, Jankiewicz O, Morales GH, Johnson C, Horbach
815 E, Hoffmann KP, Kr P, Shah R, Anderson GM, Mortimer NT, Schmitz JE,
816 Hadjifrangiskou M, Foti A, Dahl J-U. 2022. Redox-Mediated Inactivation of the
817 Transcriptional Repressor RcrR is Responsible for Uropathogenic Escherichia coli's
818 Increased Resistance to Reactive Chlorine Species. mBio 13:e01926-22.
819 40. Kitagawa M, Matsumura Y, Tsuchido T. 2000. Small heat shock proteins, IbpA and
820 IbpB, are involved in resistances to heat and superoxide stresses in Escherichia coli.
821 FEMS Microbiol Lett 184:165–171.
822 41. Lewis K. 2000. Programmed Death in Bacteria. Microbiol Mol Biol Rev 64:503–514.

823 42. Keyer K, Imlay JA. 1996. Superoxide accelerates DNA damage by elevating free-
824 iron levels. Proceedings of the National Academy of Sciences of the United States
825 of America 93:13635–13640.
826 43. Liochev SI, Fridovich I. 1994. The role of O2.- in the production of HO.: in vitro and
827 in vivo. Free Radic Biol Med 16:29–33.
828 44. Taber HW, Mueller JP, Miller PF, Arrow AS. 1987. Bacterial uptake of
829 aminoglycoside antibiotics. Microbiological Reviews 51:439–457.
830 45. Kim W, Zhu W, Hendricks GL, Van Tyne D, Steele AD, Keohane CE, Fricke N,
831 Conery AL, Shen S, Pan W, Lee K, Rajamuthiah R, Fuchs BB, Vlahovska PM, Wuest
832 WM, Gilmore MS, Gao H, Ausubel FM, Mylonakis E. 2018. A new class of synthetic
833 retinoid antibiotics effective against bacterial persisters. Nature 2018 556:7699
834 556:103–107.
835 46. Pletzer D, Mansour SC, Hancock REW. 2018. Synergy between conventional
836 antibiotics and anti-biofilm peptides in a murine, sub-cutaneous abscess model
837 caused by recalcitrant ESKAPE pathogens. PLOS Pathogens 14:e1007084.
838 47. MacNair CR, Stokes JM, Carfrae LA, Fiebig-Comyn AA, Coombes BK, Mulvey MR,
839 Brown ED. 2018. Overcoming mcr-1 mediated colistin resistance with colistin in
840 combination with other antibiotics. Nature Communications 2018 9:1 9:1–8.
841 48. Arndt-Jovin DJ, Jovin TM. 1989. Chapter 16 Fluorescence Labeling and Microscopy
842 of DNA. Methods in Cell Biology 30:417–448.
843 49. Bryan LE, Van Den Elzen HM. 1976. Streptomycin accumulation in susceptible and
844 resistant strains of Escherichia coli and Pseudomonas aeruginosa. Antimicrobial
845 agents and chemotherapy 9:928–938.

50. Nowack B, Krug HF, Height M. 2011. 120 years of nanosilver history: implications for policy makers. Environ Sci Technol 45:1177–1183.
51. Jung WK, Koo HC, Kim KW, Shin S, Kim SH, Park YH. 2008. Antibacterial Activity and Mechanism of Action of the Silver Ion in Staphylococcus aureus and Escherichia coli. Applied and Environmental Microbiology 74:2171–2178.
52. Wakshlak RB-K, Pedahzur R, Avnir D. 2015. Antibacterial activity of silver-killed bacteria: the “zombies” effect. 1. Sci Rep 5:9555.
53. Panáček A, Kvítek L, Smékalová M, Večeřová R, Kolář M, Röderová M, Dyčka F, Šebela M, Prucek R, Tomanec O, Zbořil R. 2017. Bacterial resistance to silver nanoparticles and how to overcome it. Nature Nanotechnology 2017 13:1 13:65–71.
54. Wang H, Wang M, Xu X, Gao P, Xu Z, Zhang Q, Li H, Yan A, Kao RYT, Sun H. 2021. Multi-target mode of action of silver against Staphylococcus aureus endows it with capability to combat antibiotic resistance. Nature Communications 2021 12:1 12:1–16.
55. Tambosi R, Liotenberg S, Bourbon M-L, Steunou A-S, Babot M, Durand A, Kebaili N, Ouchane S. 2018. Silver and Copper Acute Effects on Membrane Proteins and Impact on Photosynthetic and Respiratory Complexes in Bacteria. mBio 9:e01535-18.
56. Vaishampayan A, de Jong A, Wight DJ, Kok J, Grohmann E. 2018. A novel antimicrobial coating represses biofilm and virulence-related genes in methicillin-resistant Staphylococcus aureus. Frontiers in Microbiology 9:1–14.
57. Dwyer DJ, Belenky PA, Yang JH, Cody MacDonald I, Martell JD, Takahashi N, Chan CTY, Lobritz MA, Braff D, Schwarz EG, Ye JD, Pati M, Vercruysse M, Ralifo PS,

869 Allison KR, Khalil AS, Ting AY, Walker GC, Collins JJ. 2014. Antibiotics induce
870 redox-related physi. Proceedings of the National Academy of Sciences of the United
871 States of America 111:E2100–E2109.
872 58. Herisse M, Duverger Y, Martin-Verstraete I, Barras F, Ezraty B. 2017. Silver
873 potentiates aminoglycoside toxicity by enhancing their uptake. Molecular
874 Microbiology 105:115–126.
875 59. Ling J, Cho C, Guo L-T, Aerni H, Rinehart J, Söll D. 2012. Protein aggregation
876 caused by aminoglycoside action is prevented by a hydrogen peroxide scavenger.
877 Mol Cell 48:713–722.
878 60. Ye J, Su Y, Lin X, Lai S, Li W, Ali F, Zheng J, Peng B. 2018. Alanine Enhances
879 Aminoglycosides-Induced ROS Production as Revealed by Proteomic Analysis.
880 Frontiers in Microbiology 9.
881 61. Ji X, Zou J, Peng H, Stolle A-S, Xie R, Zhang H, Peng B, Mekalanos JJ, Zheng J.
882 2019. Alarmone Ap4A is elevated by aminoglycoside antibiotics and enhances their
883 bactericidal activity. Proceedings of the National Academy of Sciences 116:9578–
884 9585.
885 62. Imlay JA. 2002. How oxygen damages microbes: Oxygen tolerance and obligate
886 anaerobiosisAdvances in Microbial Physiology.
887 63. Park S, You X, Imlay JA. 2005. Substantial DNA damage from submicromolar
888 intracellular hydrogen peroxide detected in Hpx- mutants of Escherichia coli.
889 Proceedings of the National Academy of Sciences 102:9317–9322.
890 64. Poole K. 2011. Pseudomonas aeruginosa: Resistance to the max. Frontiers in
891 Microbiology 2:65.

892 65. Hancock REW, Farmer SW, Li Z, Poole K. 1991. Interaction of aminoglycosides with
893 the outer membranes and purified lipopolysaccharide and OmpF porin of Escherichia
894 coli. Antimicrobial Agents and Chemotherapy 35:1309–1314.
895 66. Hancock RE, Raffle VJ, Nicas TI. 1981. Involvement of the outer membrane in
896 gentamicin and streptomycin uptake and killing in Pseudomonas aeruginosa.
897 Antimicrobial Agents and Chemotherapy 19:777–785.
898 67. Wright GD. 2016. Antibiotic Adjuvants: Rescuing Antibiotics from Resistance. Trends
899 in Microbiology 24:862–871.
900 68. Price M, Reiners JJ, Santiago AM, Kessel D. 2009. Monitoring Singlet Oxygen and
901 Hydroxyl Radical Formation with Fluorescent Probes During Photodynamic Therapy.
902 Photochemistry and Photobiology 85:1177–1181.
903 69. Pfaffl MW. 2001. A new mathematical model for relative quantification in real-time
904 RT–PCR. Nucleic Acids Research 29:e45.
905 70. Helander IM, Mattila-Sandholm T. 2000. Fluorometric assessment of Gram-negative
906 bacterial permeabilization. Journal of Applied Microbiology 88:213–219.
907 71. Sabnis A, Hagart KLH, Klöckner A, Becce M, Evans LE, Furniss RCD, Mavridou DAI,
908 Murphy R, Stevens MM, Davies JC, Larrouy-Maumus GJ, Clarke TB, Edwards AM.
909 2021. Colistin kills bacteria by targeting lipopolysaccharide in the cytoplasmic
910 membrane. eLife 10.
911 72. Saito H, Inui K, Hori R. 1986. Mechanisms of gentamicin transport in kidney epithelial
912 cell line (LLC-PK1). Journal of Pharmacology and Experimental Therapeutics 238.
913
914

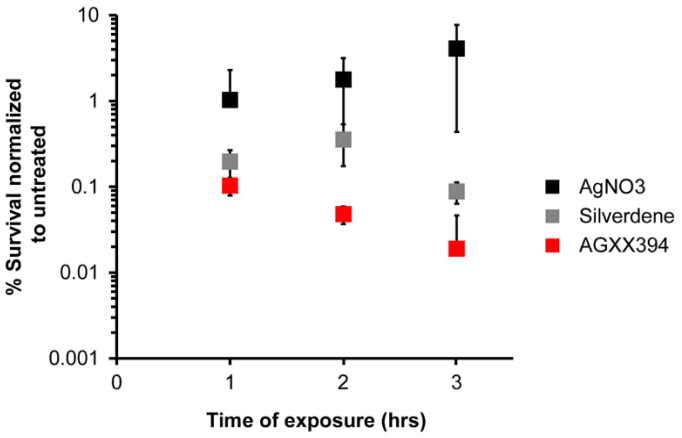

FIG 1 AGXX394 is more efficient in killing *P. aeruginosa* than silverdene and silver nitrate. Overnight PA14 cultures were diluted ~25-fold into MOPSg media (OD_{600}=0.1) and treated for three hours with 25 µg/ml $AgNO_3$ (black), silverdene (grey), and AGXX394 (red), respectively. Colony survival was evaluated every hour by serially diluting samples and plating them onto LB agar. Percent survival was calculated relative to the untreated control (*n=4, ± S.D).*

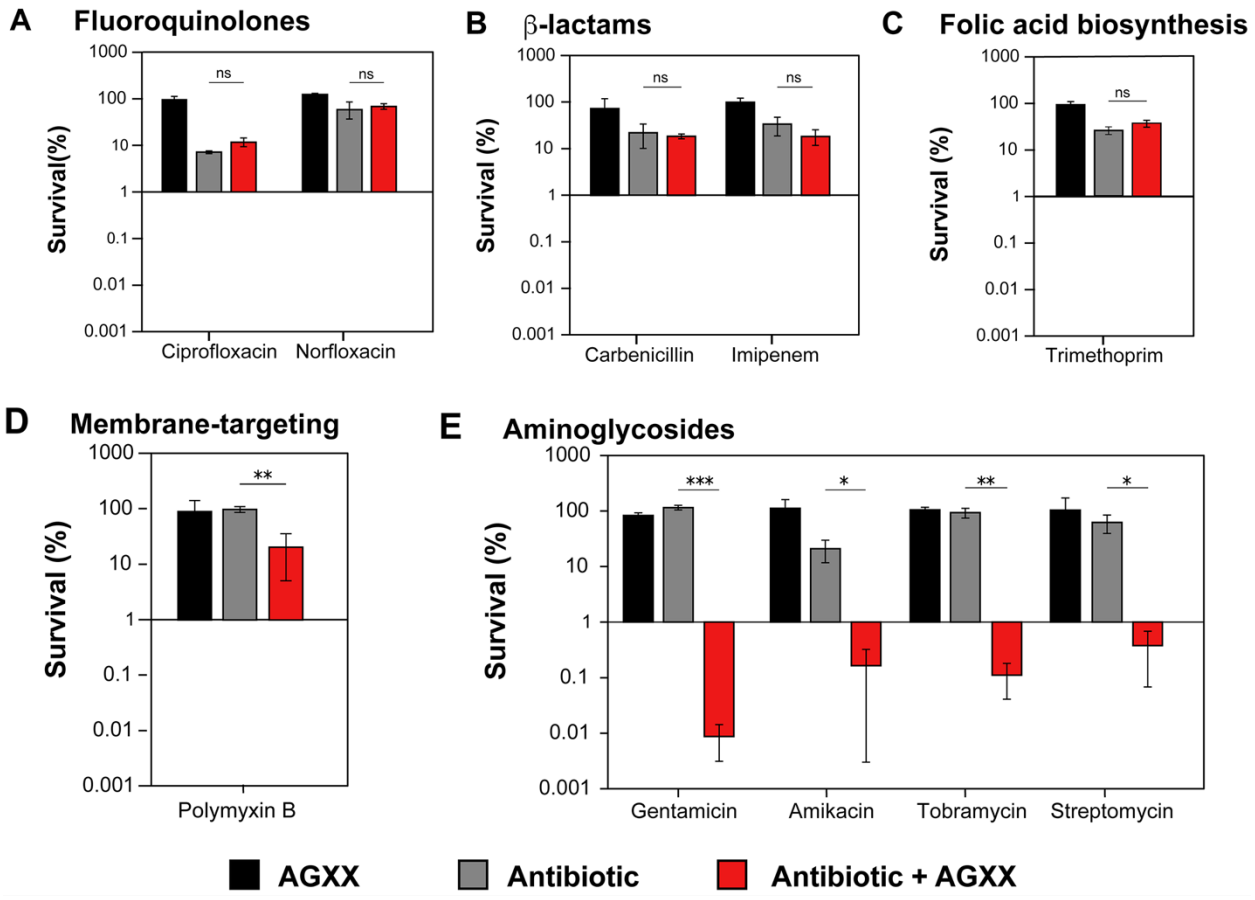

FIG 2 AGXX exponentially increases the activity of aminoglycosides against *P. aeruginosa*. Overnight PA14 cultures were diluted ~25-fold (OD_{600}=0.1) into Mueller-Hinton media and exposed to 75 µg/ml AGXX720C (black bars), a sublethal concentration of the indicated antibiotic (grey bar), or the combined treatment of both (red bars) for 3 hours. Samples were taking every 60 min, serial diluted, plated on LB agar, and incubated for 20 hours for CFU counts. Percent survival was calculated relative to the untreated control for: **(A)** 35 ng/ml ciprofloxacin and 100 ng/ml nalidixic acid, respectively; **(B)** 79 µg/ml carbenicillin and 0.156 µg/ml imipenem, respectively; **(C)** 125 µg/ml trimethoprim; **(D)** 1.5 µg/ml polymyxin B; and **(E)** 0.4 µg/ml gentamicin, 2.0 µg/ml amikacin, 1.0 µg/ml tobramycin, and 3 µg/ml streptomycin, respectively. All experiments were performed in at least three biological replicates and error bars represent mean ± SD. * $p < 0.05$, ** $p < 0.01$, *** $p < 0.001$ (Student's t test, calculated relative to cultures treated with antibiotics alone).

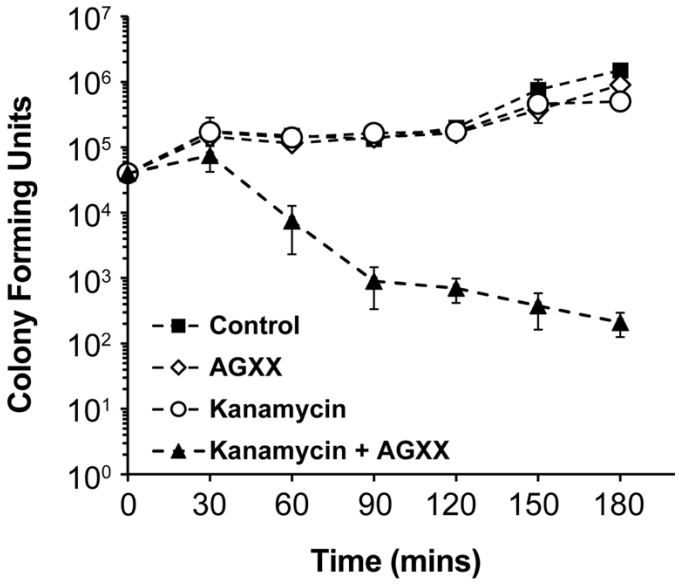

944

945 **FIG 3 AGXX increases the sensitivity of *P. aeruginosa* strain PA14 to kanamycin.**
946 Overnight PA14 cultures were diluted ~25-fold into Mueller-Hinton media (OD_{600}=0.1) and
947 either left untreated or exposed to 75 µg/ml AGXX720C, 50 µg/ml kanamycin, or the
948 combination thereof for 3 hours. Samples were taken every 30 minutes, serial diluted and
949 plated on LB agar for CFU counts, (*n=4, ± S.D)*.

950

951

952

953

954

955

956

957

958

959

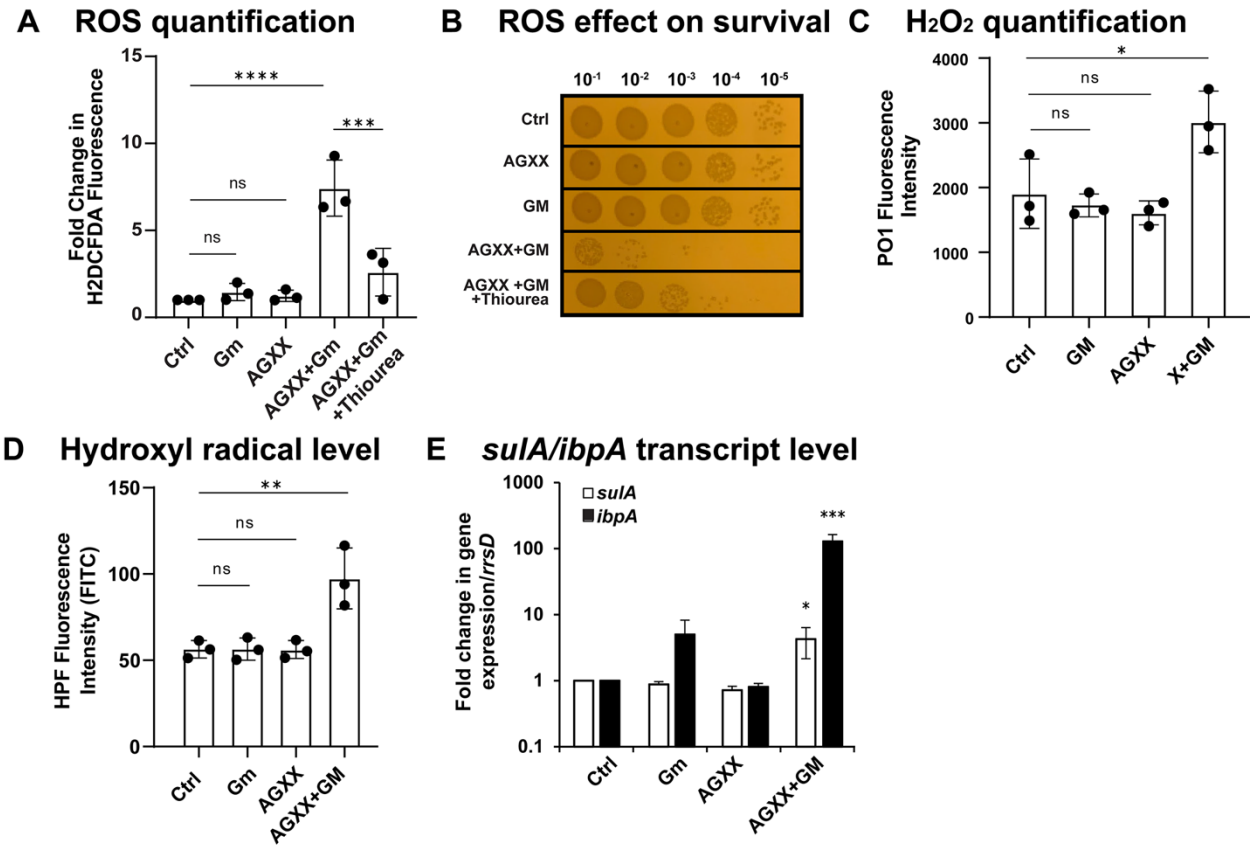

FIG 4 The combination of sublethal concentrations of AGXX and aminoglycosides increases ROS formation and causes DNA damage and protein aggregation. Mid-log PA14 cells were treated with sublethal concentrations of Gm (0.25 µg/ml), AGXX720C (50 µg/ml), the combination thereof, or left untreated. **(A)** Intracellular ROS levels were quantified by H_2DCFDA fluorescence. 50mM thiourea was used as a ROS quencher (*n=3, ± S.D)*. **(B)** Samples were serially diluted in PBS after 60 min of incubation, spot-titered onto LB agar and incubated for 20 hours. One representative of three independent experiments with similar outcomes. **(C, D)** Cells were strained with **(C)** 10 µM peroxy-orange 1 (PO1) and **(D)** 10µM hydroxyphenyl fluorescein (HPF) for 60 min and fluorescence was measured via flow cytometry (*n=3, ± S.D)*. **(E)** The induction of *sulA* (white bar) and *ibpA* (black bar) transcript levels was determined by qRT-PCR. Gene expression was normalized to the housekeeping gene *rrsD* and calculated as fold changes based on expression levels in the untreated control (*n=3, ± S.D.*). One-way ANOVA, Dunnett's posttest; *ns p>0.05, * p* < 0.05, ** *p* < 0.01, *** *p* < 0.001, **** *p* < 0.0001.

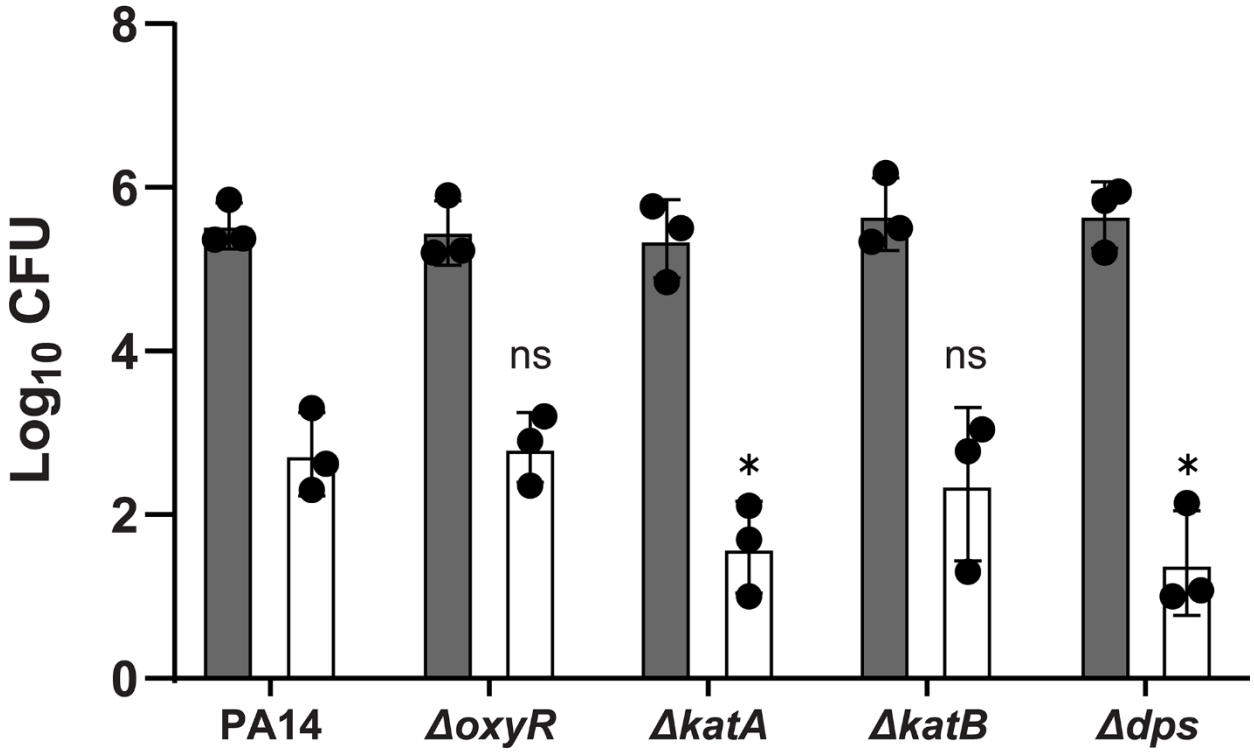

FIG 5 Antioxidant systems provide protection against ROS-mediated damage caused by a combinational treatment of AGXX and aminoglycosides. Overnight cultures of PA14 wildtype, Δ*oxyR,* Δ*katA,* Δ*katB* and Δ*dps* were diluted into MOPSg to an OD_{600}=0.01 and grown under aerobic conditions until OD_{600}=0.1. Cultures were either left untreated (grey bars) or treated with a combination of 0.25 µg/ml tobramycin and 25 µg/ml AGXX720C (white bars). Bacterial survival was quantified after two hours by serially diluting cells in PBS and plating on LB agar for 20 hours at 37°C (*n=3,* ± *S.D*). Student t-test, * $p < 0.05$).

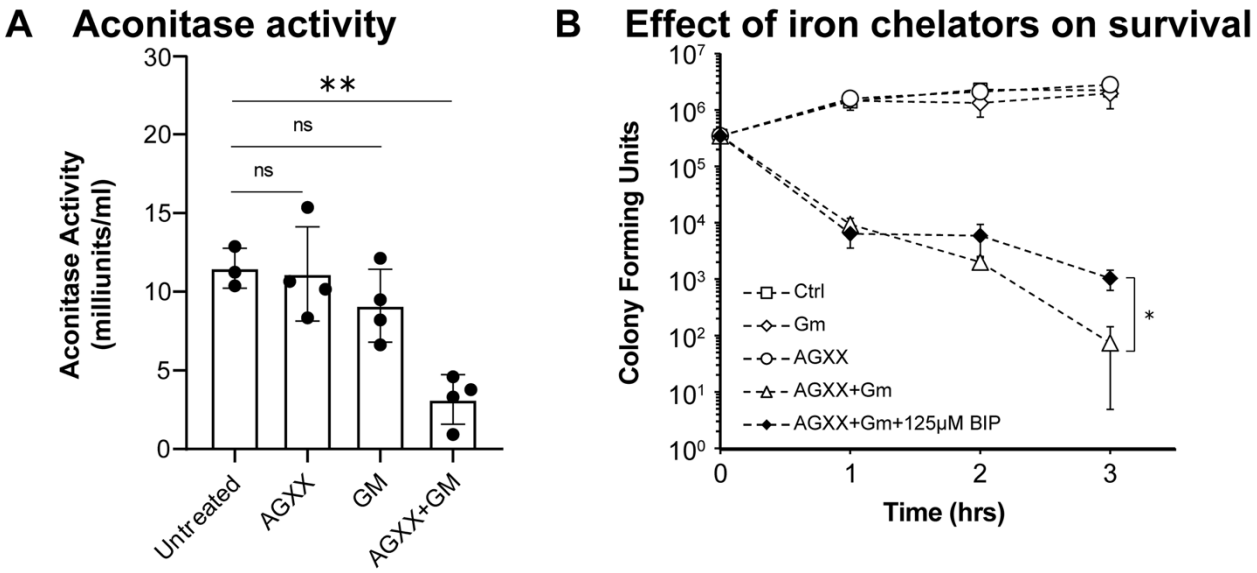

FIG 6 The synergy between AGXX and aminoglycosides on PA14 killing is in parts mediated by a disruption in iron homeostasis. Overnight PA14 cultures were diluted into MOPSg and incubated under aerobic conditions until exponential phase was reached. **(A)** Cells were left untreated or treated with 100 µg/ml AGXX720C, 0.6 µg/ml Gm, or the combination thereof for 1 hour. Aconitase activities were determined in crude extracts (*n=4,* ± *S.D*). One-way ANOVA, Dunnett's posttest; *ns p>0.05,* ** $p < 0.01$. **(B)** Cultures were either left untreated (white square) or treated with 0.25 µg/ml Gm (white diamond), 50µg/ml AGXX720C (white circle), or the combination thereof (white triangle) for three hours. Survival was determined each hour by serially diluting samples in PBS and plating onto LB agar for overnight growth. The impact of free iron on the increased killing by AGXX/Gm cotreatments was tested by the absence (white triangle) and presence (black diamonds) of 125 µM 2',2' bipyridyl (*n=3,* ± *S.D.*). Student's t test, * $p<0.05$).

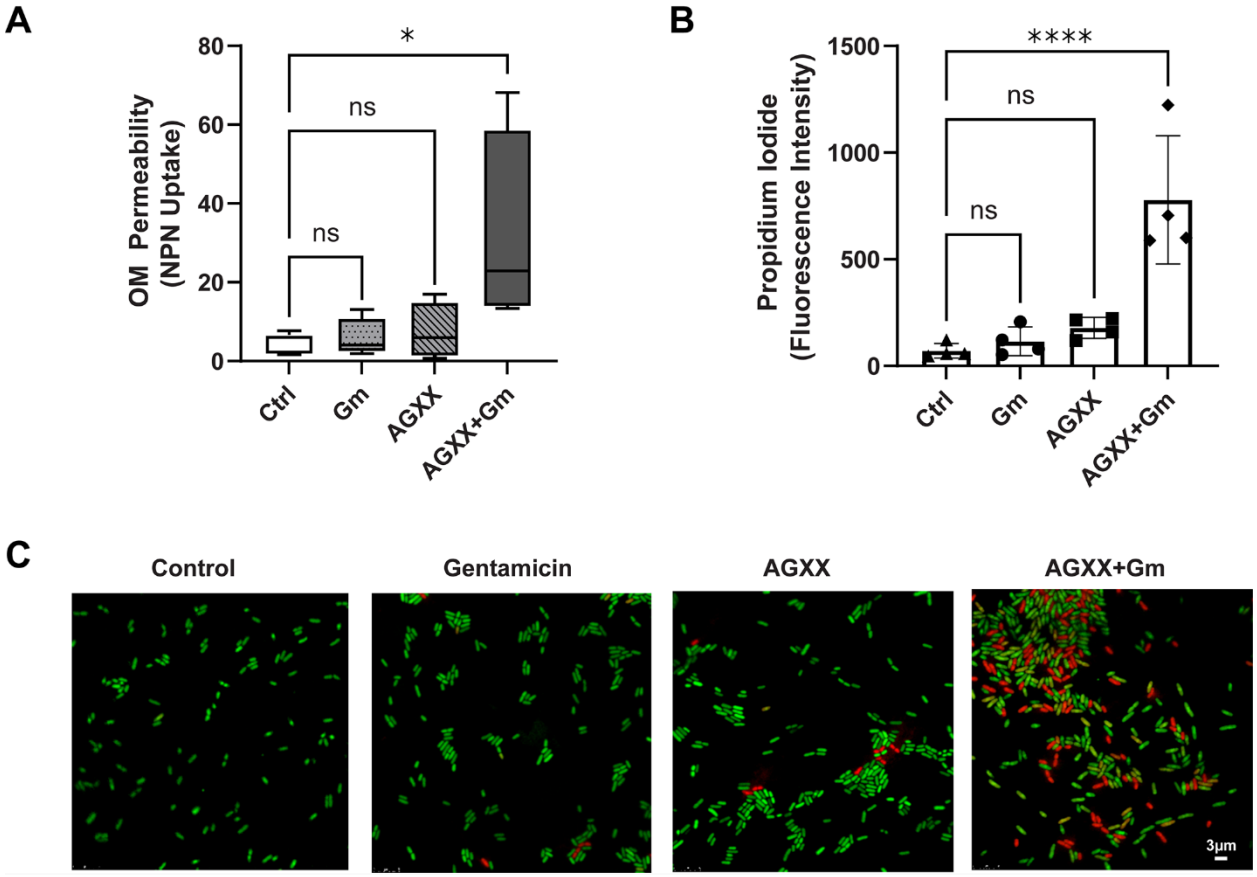

FIG 7 Combined AGXX and aminoglycoside treatment induces significant membrane damage. PA14 cells grown to mid-log phase in MOPSg media were left untreated or treated with sublethal concentrations of Gm (0.25 µg/ml), AGXX720C (50µg/ml), and the combination thereof. Cells were harvested after 1 hour of treatment, washed in PBS, and stained with **(A)** 10 µM N-phenyl-1-naphthylamine (NPN) dye, and **(B)** 0.5 µM propidium iodide (PI). Fluorescence intensities were determined at excitation/emission wavelengths of **(A)** 350/420 nm and **(B)** 535/617 nm, respectively, (*n=4,* ± *S.D.*). One-way ANOVA, Dunnett's posttest; *ns* $p>0.05$, * $p < 0.05$, **** $p < 0.0001$. **(C)** Samples were washed in PBS, stained with PI/Syto9, incubated in the dark for 15 minutes at room temperature, mounted onto a glass slide with 1% agarose, and imaged at 60x magnification via inverted confocal microscopy. One representative of three independent experiments with similar outcomes.

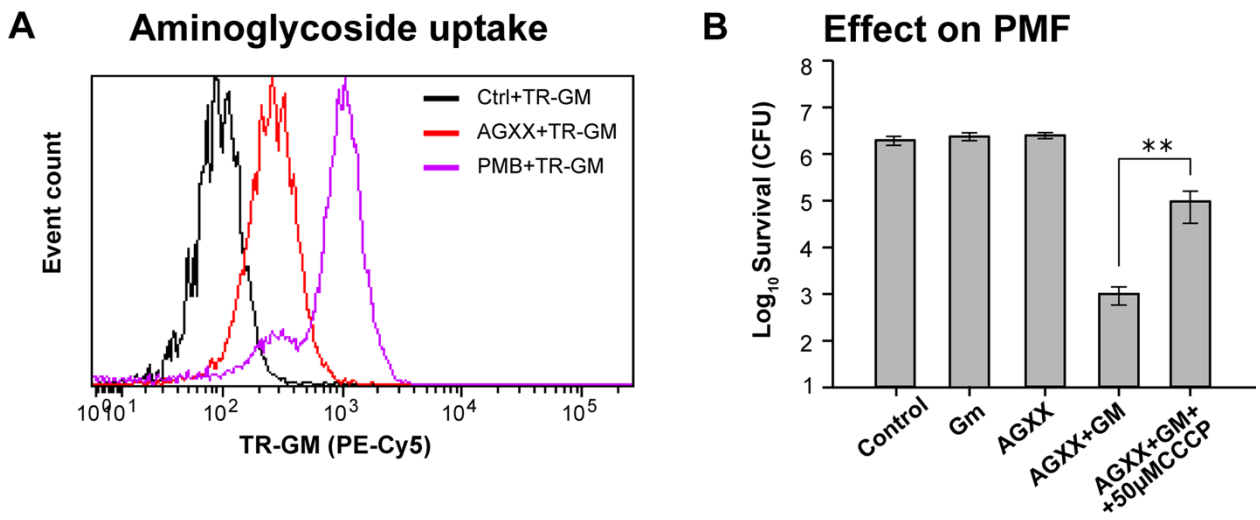

FIG 8 AGXX increases aminoglycoside uptake and lethality through increased activity of the proton motive force (PMF). (A) Mid-log PA14 cells were treated with 1.0 μg/ml TR-Gm, 1.0 μg/ml TR-Gm + 50 μg/ml AGXX720C, and 1.0 μg/ml TR-Gm + 2.0 μg/ml polymyxin B (PMB) for 1 hour, respectively. TR-Gm uptake was measured via flow cytometry. **(B)** Mid-log phase PA14 were left untreated (control) or exposed to 0.25 μg/ml Gm, 50 μg/ml AGXX720C or 0.25 μg/ml Gm + 50 μg/ml AGXX720C for 3 hours. Samples were serial diluted, plated on LB agar, and incubated for 20 hours for CFU counts. To test the impact of the PMF on the killing of a combination of AGXX and aminoglycosides, PA14 were pretreated with or without 50 μM carbonyl cyanide *m*-chlorophenyl hydrazone (CCCP) prior to AGXX/Gm exposure *(n=3, ± S.D.)*. Student's t test, ** $p<0.01$.

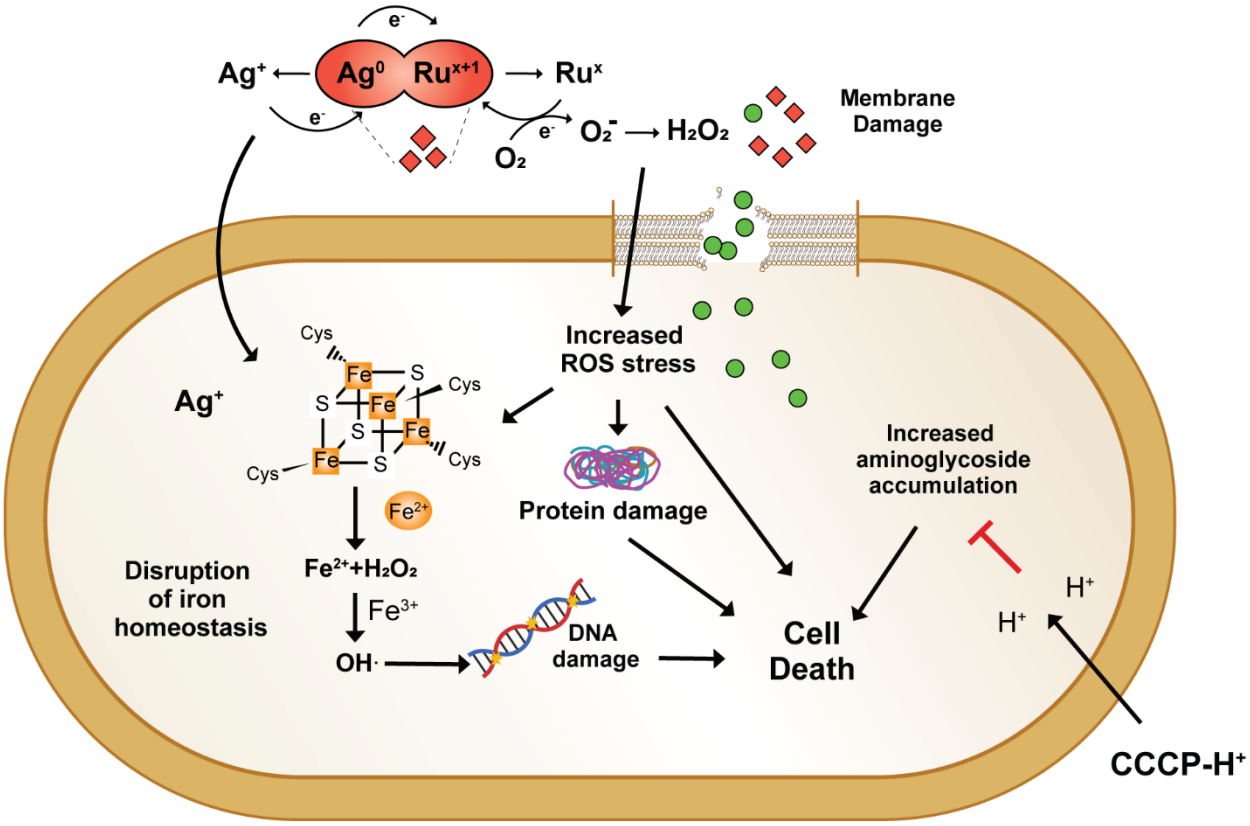

FIG 9 Proposed model for the synergy between AGXX and aminoglycoside antibiotics. The antimicrobial action of AGXX is mediated by superoxide (O_2^-) and hydrogen peroxide (H_2O_2), which are generated in a redox cycle between silver (Ag) and ruthenium (Ru^{x+1}). The combination of AGXX and aminoglycosides concertedly increases endogenous ROS levels. Potentially facilitated by a release of silver ions, the increased ROS level may disrupt iron-sulfur clusters in metabolic enzymes such as aconitase, resulting in the release of free iron, which ultimately triggers hydroxyl radical (OH•) formation in a Fenton reaction. Increasing ROS levels can inflict macromolecule damage such as DNA damage and protein aggregation, contributing to increased killing as observed for *P. aeruginosa* that were treated with a combination of AGXX and aminoglycosides. The synergistic effect between AGXX and aminoglycosides is also mediated by an increased uptake and the cellular accumulation of aminoglycosides, which can be attenuated by disrupting the bacterial membrane potential with ionophores such as CCCP.

1058 **Supplementary Information**

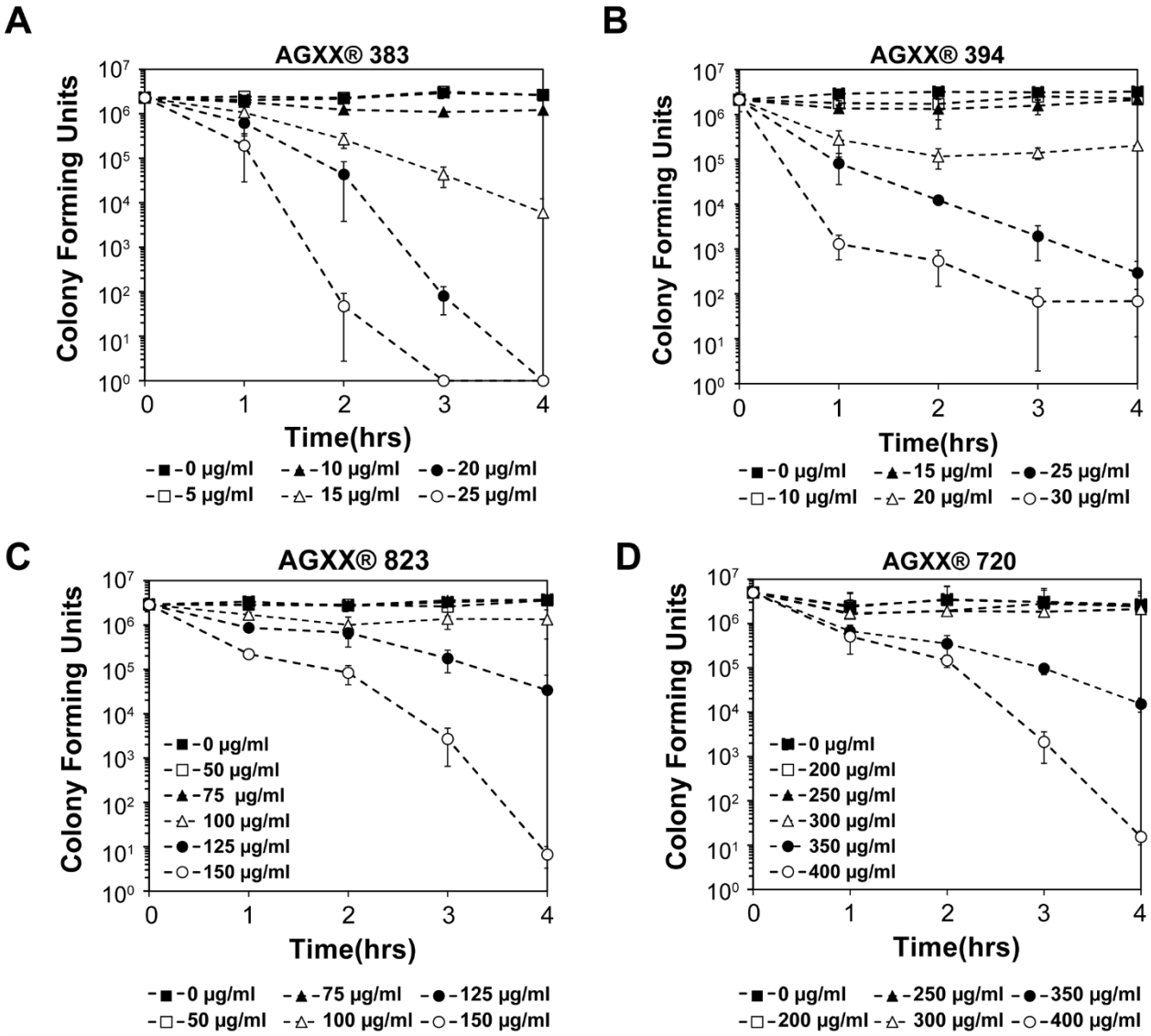

1059

1060 **FIG S1** PA14 cultures grown overnight in LB media were diluted 25-fold into MOPSg
1061 media and either left untreated (black square) or exposed to the indicated concentrations
1062 of **(A)** AGXX383, **(B)** AGXX394, **(C)** AGXX823, and **(D)** AGXX720C, respectively. For the
1063 course of four hours, samples were taken every 60 min, serial diluted, plated on LB agar,
1064 and incubated for 20 hours for CFU counts (*n=3, ± S.D.).*

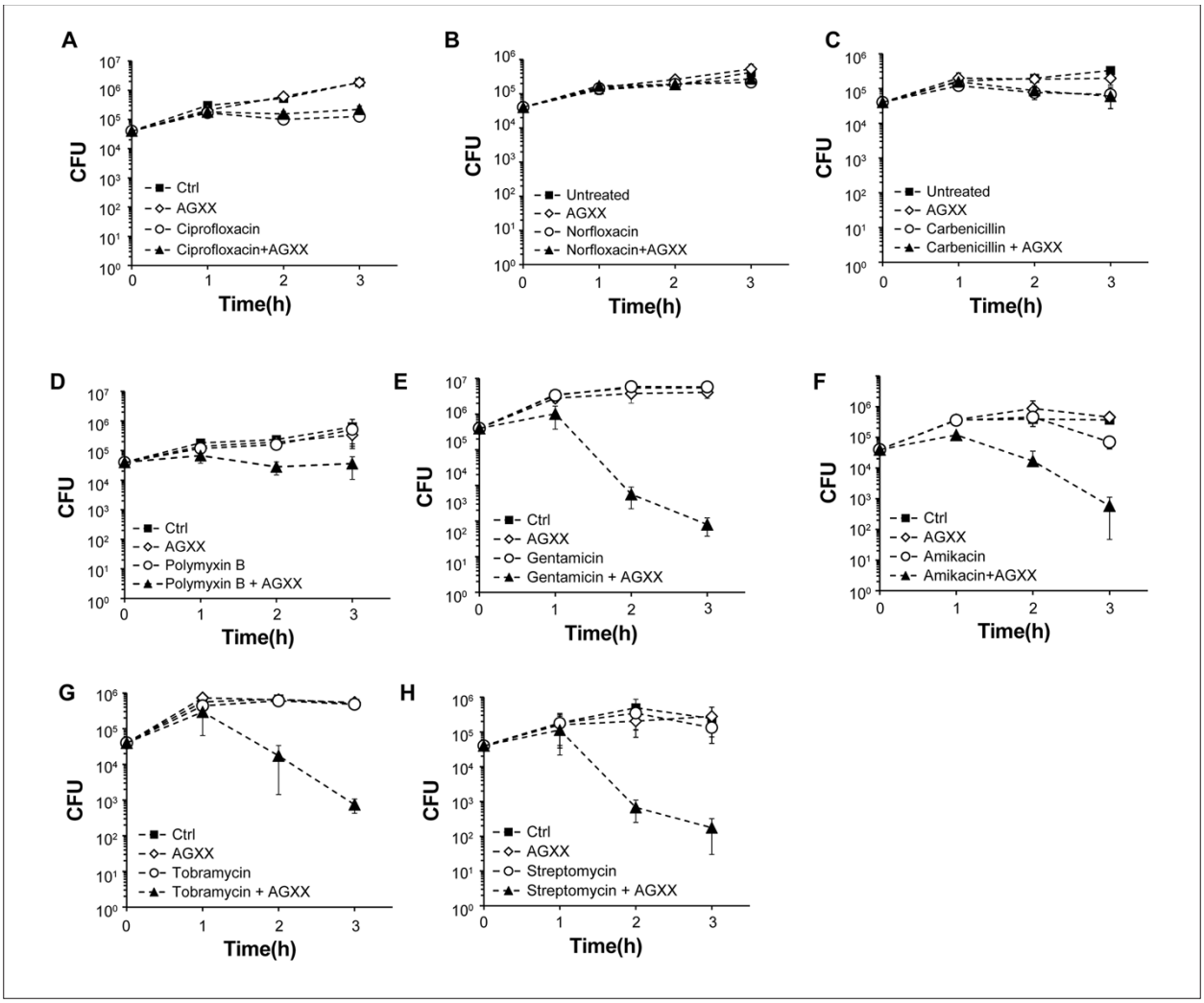

FIG S2 PA14 cultures grown overnight in LB media were diluted ~25-fold (OD_{600}=0.1) into Mueller-Hinton media and either left untreated (black square) or exposed to 75µg/ml AGXX720C (white diamond), a sublethal concentration of the indicated antibiotic (white circle), or the combination thereof (black triangle). For course of 3 hours, samples were taken every 60 min, serial diluted, plated on LB agar, and incubated for 20 hours for CFU counts (*n=3, ± S.D.).* Student's t test, ns p>0.05, * p<0.05, **** p<0.0001).

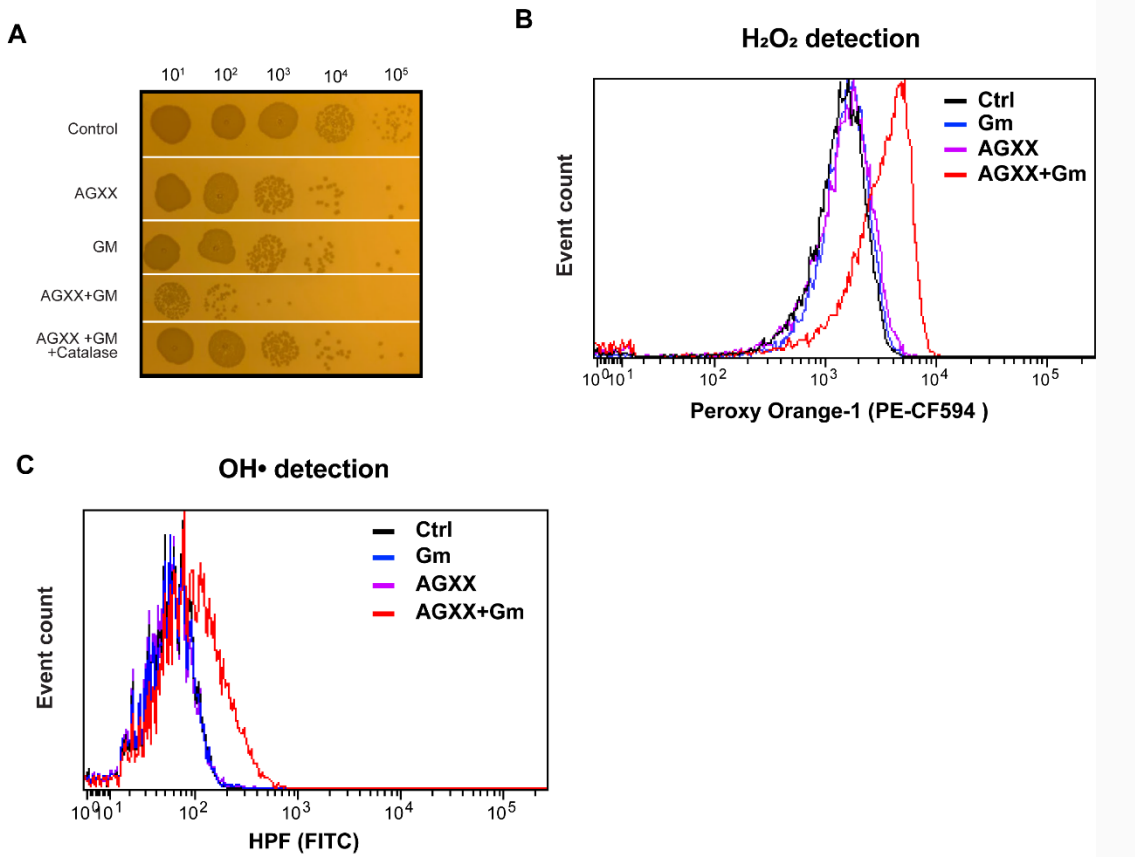

FIG S3 Combined treatment with AGXX and gentamicin increases endogenous ROS levels. (A) Mid-log PA14 cells were treated with sublethal concentrations of Gm (0.25 µg/ml), AGXX720C (50 µg/ml), the combination thereof, or left untreated. Pre-exposure to catalase was used as a ROS quencher. Samples were serially diluted in PBS after 60 min of incubation, spot-titered onto LB agar and incubated for 20 hours. One representative of three independent experiments with similar outcomes. **(B, C)** Exponentially growing PA14 cells were either left untreated or treated with sublethal concentrations of Gm (0.5 µg/ml), AGXX720C (50 µg/ml), and the combination thereof for 60 minutes. Intracellular ROS levels were quantified by staining PA14 cells with **(B)** 10 µM PO1 and **(C)** 10 µM HPF, respectively. Dye fluorescence was measured via flow cytometry after 30 min of incubation. One representative of three independent experiments of similar outcomes.

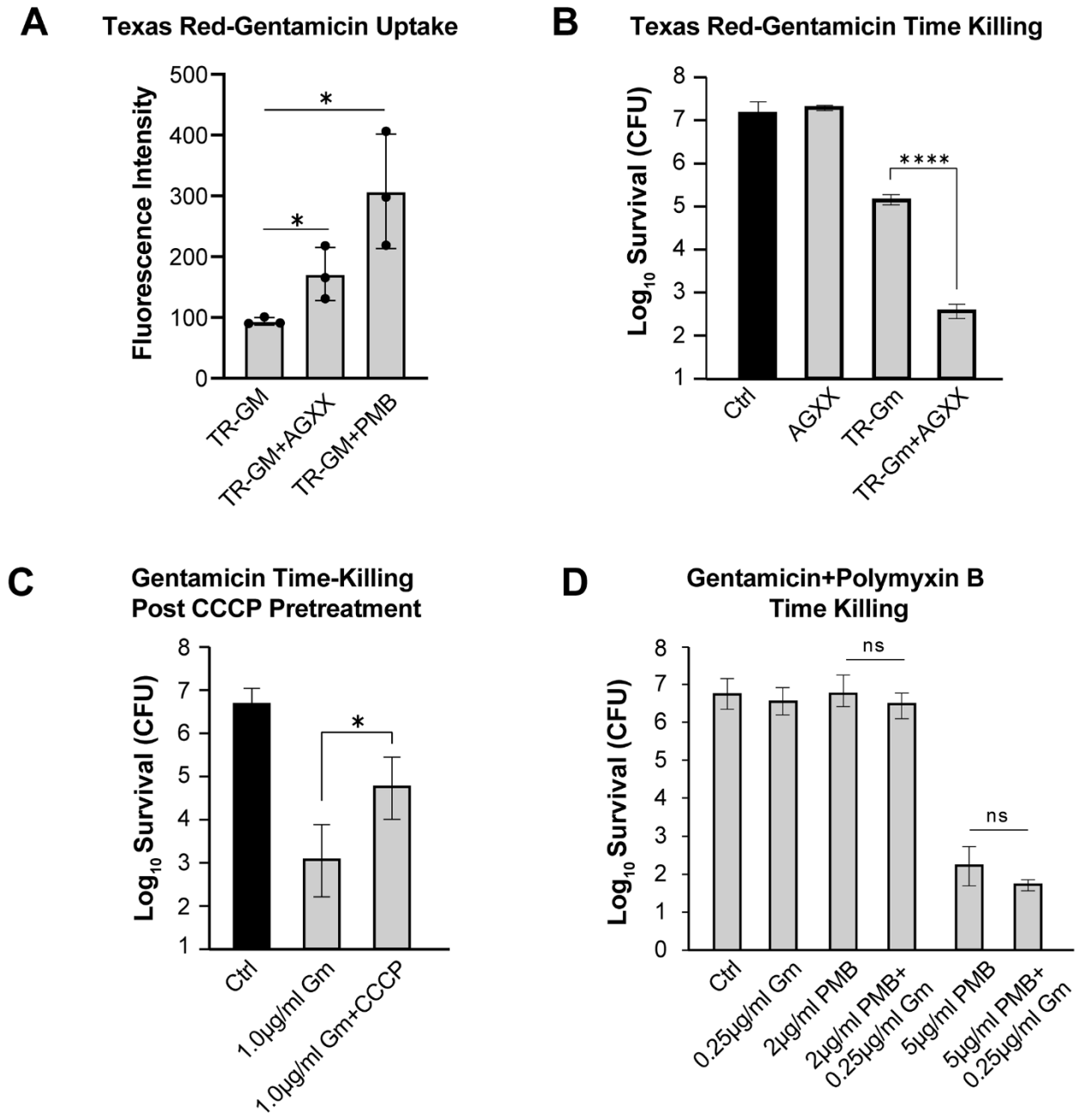

FIG S4 AGXX increases aminoglycoside uptake and lethality through increased PMF activity. PA14 cells were grown to mid-log phase (OD_{600}=0.3) and treated with: **(A)** 1.0 μg/ml TR-Gm in the presence and absence of 50 μg/ml AGXX720C and 2.0 μg/ml polymyxin B, respectively, to measure TR-Gm uptake by flow cytometry after 1 hour of treatment (*n=3, ± S.D.,)*; (**B**) 50 μg/ml AGXX720C, and 1.0 μg/ml TR-Gm in the presence and absence of 50 μg/ml AGXX720C. Samples were taken after 2 hours, serial diluted and plated on LB agar. CFU were counted after 20 hours (*n=3, ± S.D.);* **(C)** To test the

1093 impact of the PMF on the killing of 1 μg/ml Gm, cells were pre-treated with 10 μM carbonyl
1094 cyanide *m*-chlorophenyl hydrazone (CCCP) prior to Gm exposure (*n=3, ± S.D.)*; (**D**)
1095 polymyxin B (2μg/ml and 5μg/ml, respectively) with or without 0.25 μg/ml Gm for 3 hours.
1096 Samples were serial diluted, plated on LB agar, and incubated for 20 hours for CFU
1097 counts (*n=3, ± S.D.)*. (Student's t test, ns $p>0.05$, * $p<0.05$, **** $p<0.0001$).